THESIS

Björn Benedikt Sigurðarson

2023

UNIVERSITY OF VETERINARY MEDICINE BUDAPEST
DEPARTMENT OF PATHOLOGY

Hepatic cellular carcinoma in a dwarf pet rat: a case study

Björn Benedikt Sigurðarson

Supervisor: Pr. Míra Mándoki
Professor, head of department
Department of Pathology

2023

Abstract

Rats are becoming more popular as pets and understanding them as patients is essential. They are known to be prone to tumors, but liver tumors in rats are considered very rare and literature is scarce. This case study documents the pathological findings of a dyspneic dwarf pet rat with nodular liver masses. One lesion from the left liver lobe as well as two lesions from the lungs and one lesion from the bile duct were analyzed. Histopathology and immunochemistry findings were consistent with a spontaneous grade IV solid hepatocellular carcinoma, and a possible hepatic stellate cell proliferation. This type of tumors has not yet been described in pet rats and the presented findings are hoped to enrich veterinary literature and encourage deeper investigation of the dyspneic pet rat.

Absztrakt

A patkányok egyre népszerűbbek házi kedvencként, és elengedhetetlen, hogy ismerjük őket, mint pácienseket. Köztudott, hogy hajlamosak a daganatok kialakulására, de a patkányokban a májdaganatok nagyon ritkák, és az erről szóló irodalom is kevés. Ez az esettanulmány egy légzési zavarokkal küzdő, noduláris májelváltozásokat mutató törpe patkány esetét dokumentálja. A bal májlebeny egy lézióját, valamint a tüdőből és az epevezetékből származó elváltozásokat elemeztünk. A kórszövettani és immunhisztokémiai eredmények egy spontán kialakult, IV. fokozatú, szolid típusú hepatocelluláris karcinómát és egy lehetséges májcsillagsejt-proliferációt igazoltak. Ilyen típusú daganatokat - tudomásunk szerint - még nem írtak le kedvtelésből tartott patkányokban, és a bemutatott eredmények remélhetőleg gazdagítják az állatorvosi szakirodalmat, valamint a légzőszervi tüneteket mutató kedvtelésből tartott patkányok alaposabb vizsgálatára ösztönöznek.

Table of content

List of abbreviation

Acc: accessory
Cd: caudal
CdVc: caudal vena cava
CL: caudate lobe
Cr: cranial
CV: central vein
D: duodenum
DCL: dorsal caudate lobe
DRL: dorsal right lobe
ECM: extracellular matrix
FL: falciform ligament
H: heart
H&E: hematoxylin and eosin
HCC: hepatocellular carcinoma
HepPar-1: hepatocyte paraffin 1
HSC: hepatic stellate cells
Ki-67: Kiel-67
LLL: left liver lobe
LM1: lung mass 1
LM2: lung mass 2
LML: left middle lobe
MF: myofibroblast
ML: median lobe
NK: natural killer
PA: portal area
PC: paracaval
RL: right lobe
RML: right medial lobe
S: stomach
SEC: sinusoidal endothelial cells
SI: small intestines
Sp: spleen
St: sternum
TC: transverse colon
TNM: tumor node metastasis
TS: transverse septum
UVMB: University of Veterinary Medicine Budapest
VCL: ventral caudate lobe
VRL: ventral right lobe
α-SMA: alpha smooth muscle actin

1. Introduction and aims

Among exotic veterinary patients, rats are becoming more common. Fancy rats (*Rattus norvegicus domestica*) are the most commonly kept pet rats and live in average 2 years. Because they are calm, intelligent and playful, they make excellent pets [1, 2].

Rats are also easy to breed and manipulate, which make them good research models. They have been used in laboratories since the early twentieth century. In particular, they are prone to develop tumors and are the model of choice in oncology studies. Rats' short lifespan allows researchers to observe the development of tumors and the effects of treatments over a relatively short period of time. They can spontaneously develop tumors, and researchers can induce tumors in them through various methods, such as exposure to carcinogens, genetic modifications, or transplantation of tumor cells. Some strains of laboratory rats are even prone to developing specific types of tumors. For instance, the Sprague-Dawley rat is known to develop a high incidence of mammary tumors [3, 4] and is used to study mammary carcinogenesis.

While rat's short lifespan and susceptibility to tumors are advantageous for cancer research, they represent important health concerns in pet rats. The pet rat quickly becomes a geriatric patient that tend to develop tumors, mostly mammary adenomas. Interestingly, it has been found that the spontaneous dwarf rat, derived from Sprague-Dawley rats, is resistant to chemically-induced mammary tumors and lives longer [5–7]. For those reasons, certain pet rat breeders have started to focus on dwarf rat lines to offer healthier rats to their customers.

An extensive knowledge on laboratory rats' tumors has been documented in the past decades, but literature on pet rats, not to mention dwarf rats, remains scarce. Their increasing popularity makes it important to enrich veterinary knowledge on their particularities.

This study aims to document a pathology case of a dwarf pet rat diagnosed with hepatocellular carcinoma. To the best of our knowledge, this type of tumor has not yet been described in pet rats.

2. Literature review

2.1. The dwarf rat

Rats have been extensively used in scientific research for many decades due to their physiological similarities to humans, ease of handling, and well-documented biology. They are a common model organism in various fields including biology and medicine. In laboratories, one of the most commonly used strain is the Sprague-Dawley strain, developed in the early 20th century [8].

The spontaneous dwarf rat is a dwarf strain first isolated from a colony of Sprague-Dawley rats in 1977 [9, 10]. They exhibit dwarfism as they are deficient in growth hormones due to a recessive mutation making them enable to properly produce the necessary messenger ribonucleic acid for growth hormones synthesis [9, 11].

2.1.1. Special characteristics

2.1.1.1. Size and appearance

At birth, dwarf rats have similar size and weight as standard size rats (Figure 1). Until 5 weeks old (shortly after weaning), they are difficult to distinguish from standard rats. Once fully grown, dwarf rats are 40 to 75% smaller than their normal-sized counterparts and end up slightly bigger than a mouse. While adult standard rats range from 300g to 800g, dwarf rats average from 75g to 150g [12–14].

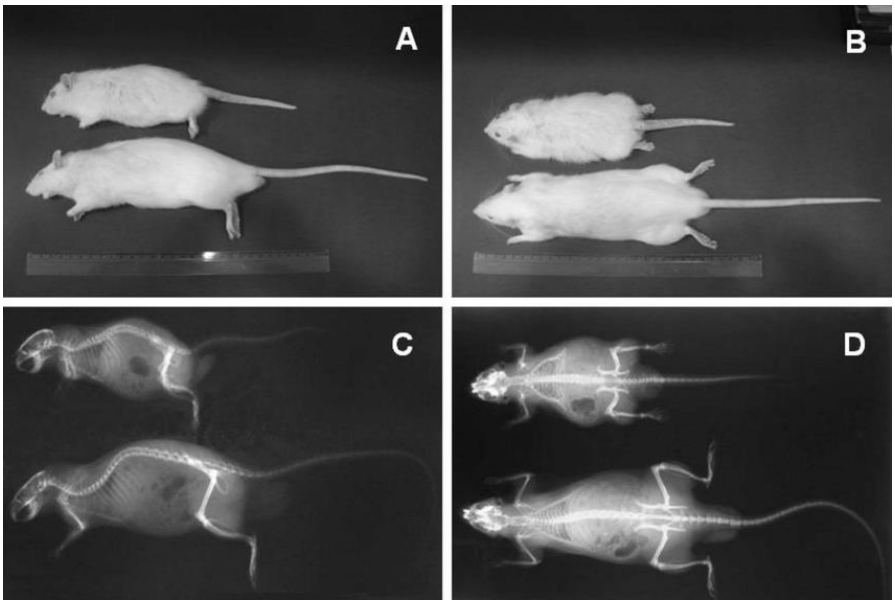

Figure 1: Comparative views of the adult size of a dwarf and a standard male rat (Andersen et al., 2009). The lateral (A) and dorsoventral (B) photographs as well as the lateral (C) and dorsoventral (D) radiographs illustrate the marked size difference

2.1.1.2. Longevity

Sexual dimorphism is not as pronounced in dwarf rats as it is in standard size rats, as male and female dwarf rats have more similar size and weight [12].

Dwarf rats have proportionally shorter tail and bigger eyes [13], which could be considered more attractive by some pet owners.

Rats live a quite short life, as their average lifespan is around 24 months [1]. However, breeders have reported longer longevity in their dwarf lines [12], which corresponds with the current scientific literature [7, 11, 15]. For instance, spontaneous dwarf rats in the aging study conducted by Kuromoto *et al.* (2010) showed an increased lifespan of 20-40% in males and 10-20% in females.

2.1.1.3. Resistance to tumors

In several studies, dwarf rats have been found resistant to certain types of tumors, including mammary gland and pituitary gland tumors. In particular, dwarf rats showed resistance to chemically induced mammary tumors [5, 6, 16]. As standard rats are particularly prone to mammary gland tumors [1, 3, 17, 18], using dwarf rats in breeding could help reduce their incidence in rats.

2.1.2. Uses

2.1.2.1. Dwarf rats in research

Dwarf rats' lack of growth hormones allows researchers to study the importance of those hormones in different physiological and pathophysiological processes. Hence, they are excellent research models including for endocrinology, aging and oncology studies. For instance, compared to standard rats, dwarf rats exert modified pituitary function [10, 11, 19], decreased body fat when exposed to normal proportionate food intake [15, 20], increased longevity [7, 11, 15], and resistance to mammary carcinogenesis [5, 6, 16].

2.1.2.2. Dwarf pet rats

Rats have been domesticated as pets since the early 1840s [21] and are derived from the Norway rat (*Rattus norvegicus*). Standard-sized fancy rats have become more and more popular pets over the last decades, especially after the release of the Disney animated movie "*Ratatouille*" [22, 23]. They make indeed excellent pets as they are very intelligent, have a gentle and calm nature and are easy to handle. If rats in general are still quite atypical pets, dwarf pet rats are even more. However, their increased longevity, body proportions (shorter tail, bigger eyes) and resistance to some tumors make them quite attractive to pet rat owners.

2.2. The rat liver

2.2.1. Liver gross anatomy

As in many other mammalian species, the rat liver is located in the cranial abdomen, in direct contact with the diaphragm, stomach, right kidney and right adrenal gland (Figure 2). In rats and other rodents, it comprises a quite large percentage of the total body mass with an average of 10g liver for a 250g rat, or around 4% [8, 24]

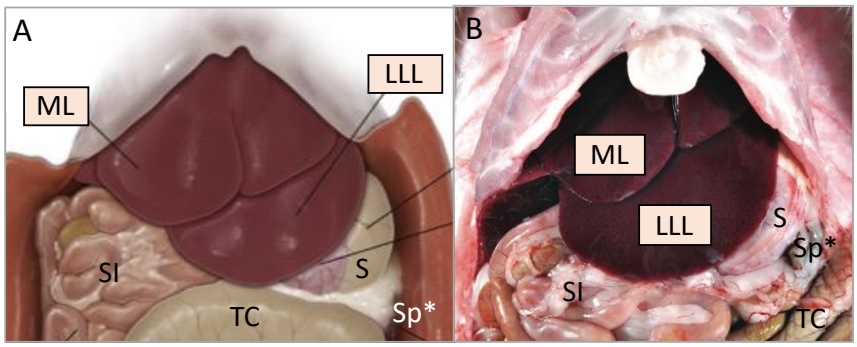

Figure 2: Regional anatomy of the rat liver
A: Schematic position of the rat liver (Treuting, 2018). B: In situ view of the rat liver (Stan, 2018).
ML: median lobe, LLL: left lateral lobe, SI: small intestines, TC: transverse colon, S: stomach, Sp*: spleen (*partially hidden)

Rats liver is composed of four anatomical lobes: right, median, left and caudate lobes [8, 24, 25] (Figure 3). The right lobe (RL) has a transverse septum that nearly bisect it, subdividing it into dorsal (DRL) and ventral (VRL) right lobes. The median lobe (ML) is the largest lobe in rats and lies most ventrally. It is subdivided by a deep fissure (main fissure or umbilical fissure) into two portions: a small left middle lobe (LML) and large right medial lobe (RML). The gallbladder, found in some other species near the median lobe, is absent in rats. Each lobe is instead being drained by its own bile duct and the common bile duct is formed by the union of the main hepatic ducts [25]. The left lobe, also referred as left lateral lobe (LLL) is located in the left part of the epigastric region, covering most of the stomach, cranial to the caudate lobe and slightly dorsal to the median lobe. It is the only rat liver lobe which is not subdivided. It presents a narrow pedicle bound with the intrahepatic vena cava [25]. The caudate lobe is located ventral to the LLL and on the left part of the vena cava. It is small and divided into a dorsal caudate lobe (DCL) and ventral caudate lobe (VCL) [24]. The VCL has a narrow pedicle lying on the ventral surface of the stomach and covered by the omentum. The DCL lies dorsal to the stomach, close from the left (gastric lobe) pancreas and the spleen. Both VCL and DCL are covered the lesser omentum, respectively its ventral and the dorsal layer.

The rat liver is attached to the diaphgram and ventral abdominal wall by the falciform ligament (*ligamentum falciforme*) (Figure 3D), from which detaches the round ligament (*lig. teres hepatis*) in its free margin. The liver coronary ligament (*lig. coronarium hepatis*) attaches the bare area (*area nuda*) of the liver to the diaphragm and forms triangular ligament (*lig. triangularia)*. The right portion of the triangular ligament (*lig. triangularia dextra*) connects the RL to the diaphragm, and its left portion (*lig. triangularia sinistra*) connects the LLL to the diaphgram. Between the LLL and the DCL, an interlobular ligament is present (Figure 3D).

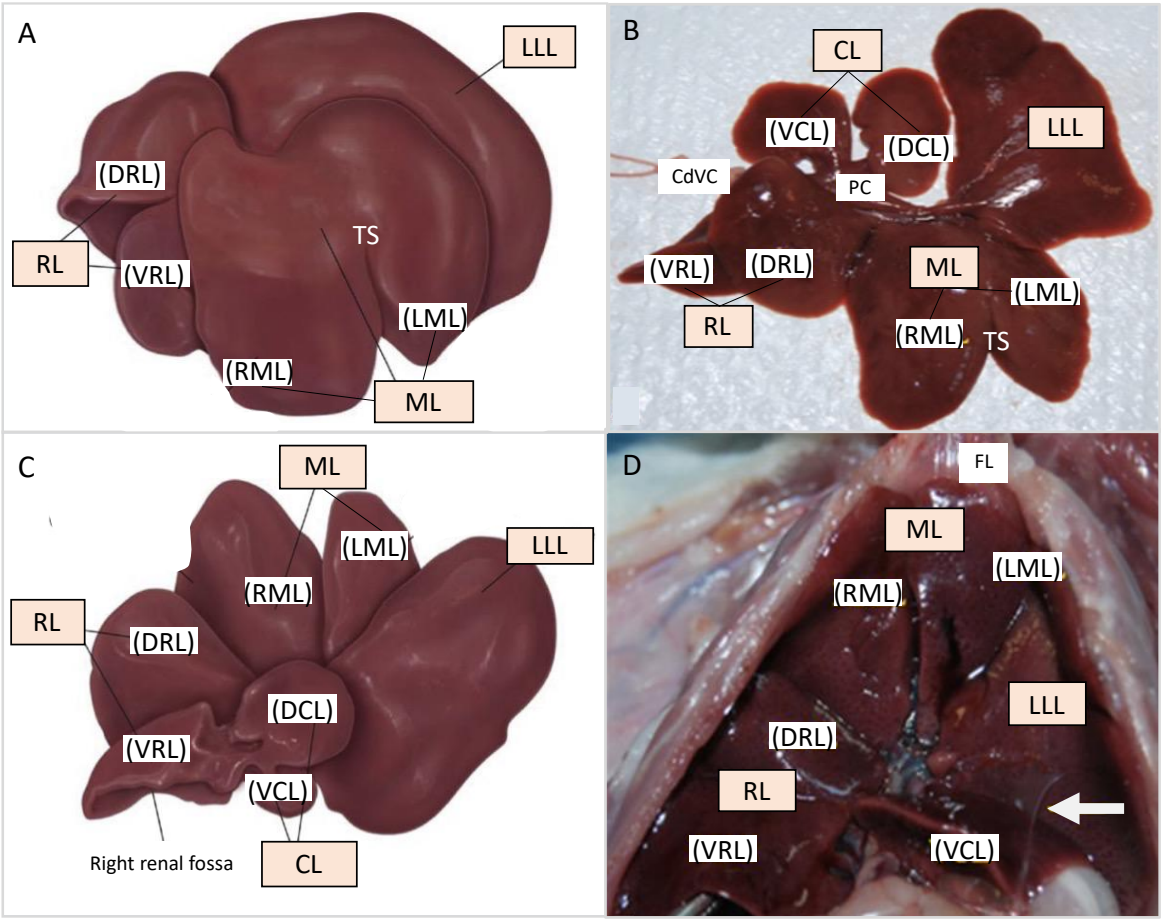

Figure 3: The rat liver lobes
A: Schematic parietal surface (Treuting, 2018), B: In situ parietal surface (Stan, 2018)
C: Schematic visceral surface (Treuting, 2018), D: In situ visceral surface (Stan, 2018).
RL: right lobe, DRL: dorsal right lobe, VRL: ventral right lobe, ML: medial lobe, LML: left median lobe, RML: right medial lobe, TS: transverse septum, LLL: left lateral lobe, CL: caudate lobe, DCL: dorsal caudate lobe, VCL: ventral caudate lobe, arrow: interlobular ligament, FL: falciform ligament, PC: paracaval portion, CdVc: caudal vena cava

2.2.2. Liver histology

2.2.2.1. Lobules and acini

When first looking at a histological slide from a cross section of a healthy rat liver, most structures resemble the ones of others domestic species. While the hepatic lobules constitute the anatomical unit of the liver, the portal lobule and hepatic acini are functional units.

The hepatic lobules have an hexagonal-like shape. In rats, those units are not outlined by connective tissue, which can make their borders more difficult to identify [26]. A central vein can be found at the center of it and portal areas are found at most corners [26, 27] (Figure 4). The hepatic lobule is known as the anatomical unit of the liver.

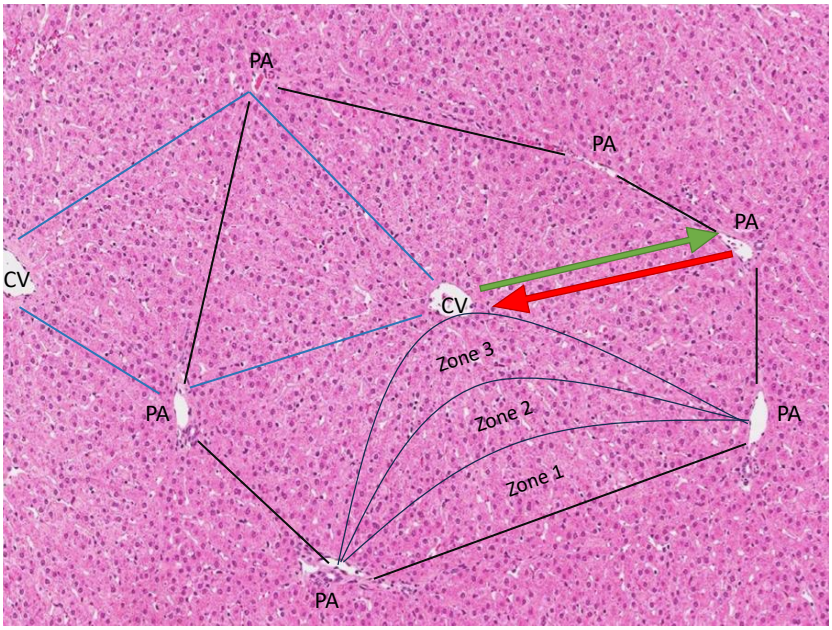

Figure 4: Histopathology of the healthy rat liver (adapted from Maynard et al., 2019)
CV: central vein, PA: portal area. One hexagonal hepatic lobule is limited by black lines. The blue lines mark the borders of a hepatic acinus and the curve lines the zones of another hepatic acinus. The green and red arrows respectively indicate the bile and blood blows within the hepatic lobule.

The central vein collects the blood that runs through the lobule, which gets directed into the hepatic vein, exiting the liver [26, 27].

The portal area is composed of 4 structures: the interlobular portal venule, interlobular hepatic arteriole, the bile ductule and the lymph capillary. The interlobular portal venule receives the blood from the digestive system and the interlobular hepatic arteriole the oxygenated blood from the hepatic artery. The bile ductule transports the bile from the liver to the common bile duct, which empties in the duodenum [26]. The lymph capillaries directs the lymph to larger lymph vessels that exit into the porta of the liver and into the hepatic lymphnodes [27].

The portal lobule is a triangular functional structure of the liver, with central veins in each corner and portal area in the center. It is based on the bile flow [27] (Figure 5).

The liver acinus is a diamond or oval shaped unit opposing 2 central veins on the long axis and 2 portal areas on the short axis. It is divided into 3 zones based on the nutrient supply. The periportal area (zone 1) is the closest to the portal area and has the best nutrient supply and more active metabolism. The pericentral area (zone 3), has the lowest supply and is hence the most vulnerable to oxygen and nutrient shortages [27–29]. The midzonal area (zone 2) is located between the periportal and pericentral areas (Figure 4, Figure 5).

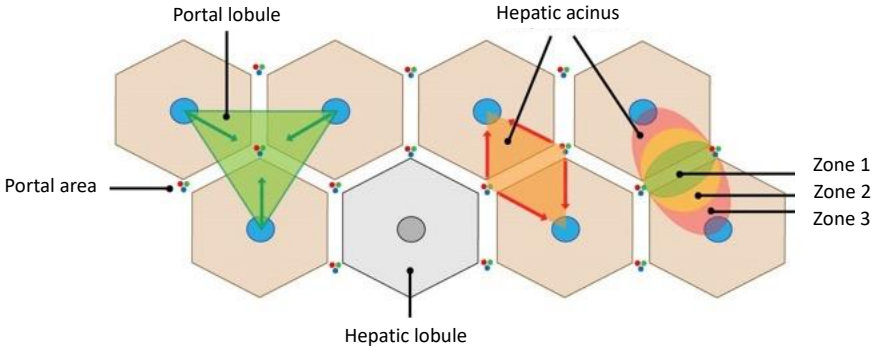

Figure 5: Structural and functional organization of the liver (aasld.org, 2020)

2.2.2.2. Hepatic plates, sinusoids and space of Disse

Hepatic plates form continuous one-cell-thick layers of densely packed hepatocytes, comprising the majority of liver structure. The hepatocytes, metabolically active cells of the liver, are organized in parallel rows and form the hepatic plates supported by collagen fibers. The hepatic plates radiate from the central vein towards the portal areas, ramifying as they approach the periphery of the hepatic lobule. In a healthy liver, each hepatic plate is separated by a sinusoid (Figure 6) [27, 28].

In between adjacent hepatocytes, bile canaliculi can be found. Within these canaliculi bile flows towards the portal area. Tight junctions and desmosomes between the hepatocytes ensure structural integrity, keeping the bile from spilling into the intercellular space [27].

Sinusoids are vascular spaces forming a complex branching network within the hepatic lobule. The ramification ensures at least one contact point with each hepatic cell. Positioned between hepatic plates, they extend from the portal area towards central vein. Blood from afferent branches of the portal area, consisting of approximately 25 % of oxygenated blood from the interlobular hepatic arteriole and 75% from the nutrient rich brood of the interlobular portal venule, mixes in the sinusoids and flows toward the efferent central vein [28].

The sinusoids are lined with specialized cells known as sinusoidal endothelial cells (SEC) which are loosely connected to one another, making the sinusoid fenestrated. This ensures that while blood cells stay within the sinusoid, blood plasma flows undisturbed towards the hepatic plate, allowing substance exchange [26–28].

Within the sinusoids, various types of blood cells can be found. In addition, so called Kupffer cells, which are specialized immune cells, can be found. These Kupffer cells are part of the monocyte-macrophage system and provide the first line of defense from harmful substances entering the liver [27]. Kupffer cells can be recognized by their angular nucleus [26]. So called pit cells, which are liver specific natural killer (NK) cells can be spotted as well, although they cannot be recognized with hematoxylin and eosin (H&E) staining [26].

The space between the hepatic plates and sinusoids is known as the space of Disse or perisinusoidal space and contains hepatic stellate cells (HSC) (Figure 6). HSC serve various functions, including nutrient storage and extracellular matrix production [26–28]. This microenvironment plays a role in nutrient exchange and detoxification and is also closely associated with the lymphatic system, where the lymph flows in the opposite way of the blood towards the portal area [26–28, 30]. This space is challenging to observe with conventional light microscopy, but special silver staining techniques can make it visible. Electron microscopy on the other hand provides a clear view of the space of Disse [26].

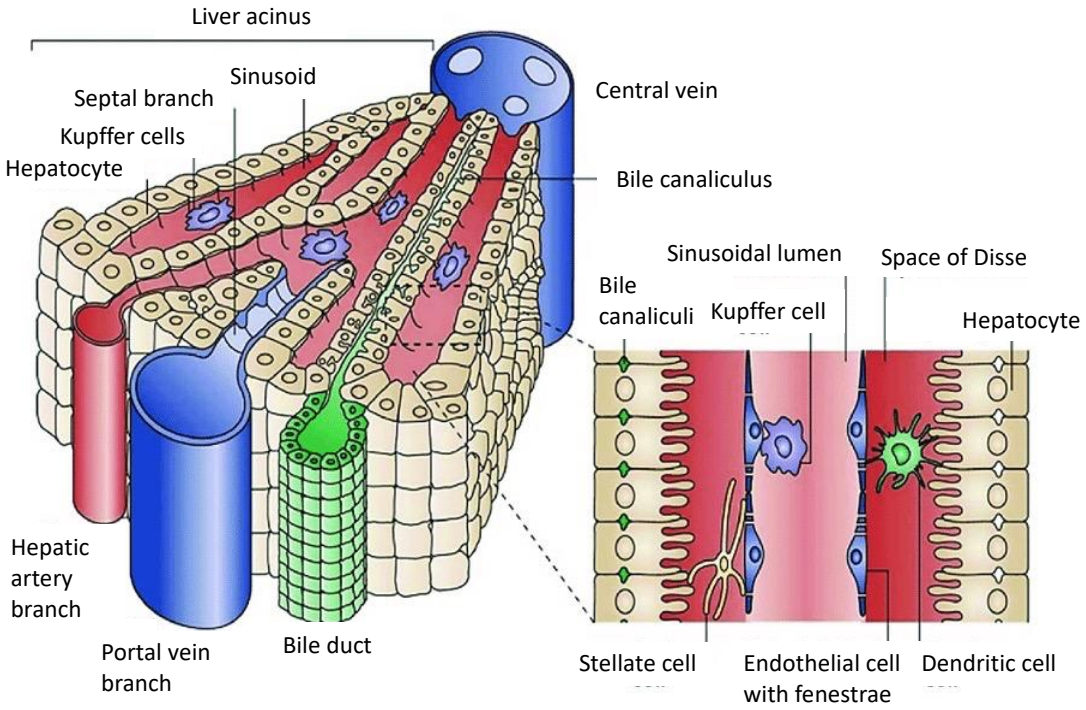

Figure 6: Structures of the liver lobule and liver sinusoids (Panwar, 2021)
The hepatocytes are aligned radially forming hepatic plates along with the sinusoids. The portal veins and hepatic artery branches terminate in the sinusoids. The space of Disse is located between the liver plate and the sinusoids and contains extracellular matrix component and stellate cells.

2.2.2.3. Hepatocytes

Hepatocytes form the parenchyma of the liver. They are specialized epithelial cells that make up about 80% of the liver volume. They have a polygonal shape. Their microvillous surface projects into the fluid filled space of Disse, their basolateral surface faces the bile canaliculi and their contact surface faces the adjacent hepatocytes, connected by tight junctions and desmosomes [27]. They have one centrally located round nucleus but seeing binucleated cells in limited number is not considered abnormal. The turnover of hepatocytes is in the medium range, so mitotic figures can be expected to be seen. Indeed, in a young rat, 1-2 mitotic figures can be expected per section, and the average lifespan of hepatocytes is around 150 days [26]. The cytoplasm can be granular in appearance, due to glycogen storage, or vacuolated due to lipid storage [27]. Bile pigments may be spotted, as fine yellow granules [27]. In an ordinary section, bile canaliculi are typically not seen [26].

Hepatocytes have a high metabolic activity and are responsible for a wide variety of functions, including production of bile, metabolism of carbohydrates, fats and proteins, synthesis of protein and urea, metabolism of xenobiotics where cytochrome P450 enzyme plays a major role, and partake in inflammation response by production of acute phase proteins [28]. Function of hepatocytes is not uniform throughout the hepatic lobule but determined by oxygen and nutrient gradient. The oxygen rich periportal zone has hepatocytes more specialized for oxidative functions such as cholesterol synthesis and β-oxidation, while the oxygen deprived pericentral area tends to perform actions such as glycolysis and metabolize xenobiotics [31].

2.2.2.4. Myofibroblasts

Liver myofibroblasts (MF) are involved regenerative processes, such as fibrosis. Three types of myofibroblast-like cells have been described in rat liver, based on location and immunohistochemical profiles: the portal MF from the portal areas, the interface MF between the parenchyma and stroma of the portal areas, and the activated hepatic stellate cells [32]. Activated hepatic stellate cells are considered the most important fibrogenic cells in the liver and stain positive for α-SMA, vimentin and desmin. Portal and interface MF are α-SMA, vimentin positive, but desmin negative [33].

2.2.2.5. Hepatic stellate cells

Hepatic stellate cells (HSC), also referred as Ito cells, lipocytes, arachnocytes or vitamin A storing cells, are liver specific pericytes from mesenchymal origin. They are located in the space of Disse and associated with SEC and hepatocytes. In physiological condition, HSC are in an inactive or quiescent state, during which they maintain homeostasis of retinoids,

chemical compounds derived from or related to vitamin A. HSC store retinoids in lipid droplets within their cytoplasm and are hence sometimes referred as lipocytes [34]. They are estimated to store 80% of total retinoids in the body [34]. They connect with surrounding hepatocytes and SEC through processes resembling stars (stellate cells) or arachnids (arachnocytes) [35]. Those processes have numerous micro projections themselves [36]. The connection to SEC is well established as the processes wrap around the sinusoids, similarly to how podocytes wrap around capillaries [28]. If direct connection with either cell type is not established [35] or if the HSC receive chemotactic signals [36], the stellate cell can activate. This happens for instance in case liver damage. During activation, the retinoid storage is lost, and intense proliferation starts, followed by phenotypic transformation into fibroblast/myofibroblast-like cells. These cells can both contract and produce a large amount of extracellular matrix (ECM), primarily in form of collagen (type I, II, IV), proteoglycans and glycoproteins [34]. Both actions lead to narrowing of the sinusoids. The structural arrangement of the ECM signals the stellate cells to either continue their differentiation or to revert to their primary inactive state [34].

Activated HSC express α-smooth muscle actin (α-SMA), which is usually found in smooth muscle cells [28, 37] and can be used as a marker to identify this phenotype (α-SMA staining). In rats, α-SMA is considered as an indicator of activated HSC, with increased upregulation showing increased contractility, but quiescent HSC show negative or mildly positive pattern [32, 38]. Interestingly, dogs show α-SMA expression in both states, where Ijzer *et al*. have suggested a more active blood flow regulation in hepatic sinusoids of dogs.

The liver is known to have good regenerative capabilities. The HSC play a significant role in that process. HSC activate, proliferate intensely and migrate towards the injury through paracrine and autocrine signaling [39]. It has been observed that after partial hepatectomy in rats, the hepatocytes proliferate with the highest intensity in the early phase of regeneration, forming avascular clusters, but not structural cords. During this phase, activated HSC produces growth factors, including hepatocyte growth factor and vascular endothelial growth factor, which stimulates the proliferation of hepatocytes. In later stages of regeneration, HSC secretes transforming growth factor-β which slows down the hepatic cells proliferation [40]. HSC hence regulate the proliferation of hepatocytes.

In the later stage of regeneration, SEC proliferate and migrate into the clusters forming the systemic histological construction seen in healthy liver [41]. It is suggested that HSC projections, that stretch in between clustered hepatocytes, enable SEC migration and the formation of sinusoids [42]. Degradation and remodeling of the (ECM) is as well regulated

by the HSC. During the early stages of regeneration, HSC inhibit the degradation of the ECM, by secreting metalloprotease inhibitors. Later on, HSC produce metalloprotease involved in the remodeling of the ECM providing structural support to the newly regenerated tissue [40].

At the last phase of the healing process, HSC undergo a transition to a senescent state. This transition is marked by a decrease in their proliferation rate and production of ECM, and an increase matrix-degrading enzymes production [40]. Additionally, cytokines are actively secreted and modulate the host's immune response. Notably, there is an upregulation of NK cell receptors, which triggers NK cell-mediated elimination of HSC. This orchestrated mechanism serves a crucial purpose in clearing HSC to prevent the development of extensive scarring and fibrosis within the liver tissue [43].

In case of severe or chronic liver injury, the activation of HSC can become continuous. In that case, excessive ECM matrix production will shield the HSC from the NK-cell activity [44]. This can lead to fibrosis, a pathological accumulation of ECM primarily in the form of collagen. Progression of fibrosis leads to vascular resistance within the liver due to narrowing of the sinusoids (sometimes called capillarization of sinusoids) which increases the pressure in the protal vein. This phenomenon is called intrahepatic portal hypertension. This restricts the blood flow to the liver and decreases metabolic and excretory function of the liver [28]. Portal hypertension can lead to opening of collateral vessels allowing the blood to bypass the liver, or acquired portosystemic shunt [28].

While liver fibrosis can be reversible, if prolonged it can lead to irreversible cirrhosis, decreasing the regenerative capabilities and function of the liver and potentially leading to hepatocellular carcinoma (HCC) [28]. Continuously activated HSC are capable of infiltrate the HCC stroma, and influence the tumor microenvironment through secretion of ECM proteins. The tumor microenvironment provided by HSC contains the same factors that contribute to the liver regeneration, but in this case support some of the hallmarks of cancer tumorigeneses. These include growth factors promoting increased proliferation and growth of hepatocytes, as well as tissue invasion and metastatis. Vascular growth factors supporting neoangiogenesis ensures supply of nutrients to cancer cells [45].

2.2.3. Liver diseases in rats

As rats have been used in laboratories for decades, a fair knowledge of their diseases has been documented. However, literature about pet rat diseases remain scarce. To the best of our knowledge, most of the recent veterinary books do not include a liver diseases chapter when considering pet rats, but laboratory and pathology books decribe hepatocellular

conditions in rats. Those include bacterial and viral hepatitis, hepatobiliary neoplasia and other miscallenous conditions such as copper accumulation in certain rat strains [2]. Liver diseases in laboratory rats are mostly experimentally induced and rarely spontaneous conditions.

2.2.3.1. Infectious hepatitis

Althought a quite rare condition, bacterial hepatitis can occur in rats. Disseminated infections caused by bacteria such as *Corynebacterium kutscheri, Staphyloccocus aureus, Clostridium piliforme* and others can lead to hepatic abscess formation and tissue necrosis in the liver. In laboratory rats, *Helicobacter* species including *H. bilis, H. typhloniui H. hepaticus, H. rodentium* can cause similar lesions in immunodepressed animals [2, 8].
In wild rats, hepatitis E is a subclinical disease and only rats experimentally infected with human hepatitis E show liver lesions [2, 46, 47]. Spontaneous viral hepatitis in rats is hence not considered likely [2].

2.2.3.2. Liver tumors

Liver tumors are infrequent in pet rats [2], but they are prevalent in laboratory rats that are intentionally exposed to different harmful substances. Long-Evans cinnamon-like colored rats have been inbred to spontaneously develop liver tumors such as hepatocellular carcinoma (HCC), and make very good models in HCC research [34]. Primary liver tumors in rats can manifest as hepatocellular adenoma, hepatocellular carcinoma, and cholangiocarcinomas, sharing similar characteristics with liver tumors observed in other companion animal species. Spontaneous occurrences of lymphosarcoma and histiocytic sarcoma often involve the liver, leading to the formation of neoplastic cell clusters in the periportal and sinusoidal regions [2].

2.3. Hepatocellular carcinoma and stellate cells tumor in domestic animals

2.3.1. Hepatocellular carcinoma

2.3.1.1. Incidence

Hepatocellular carcinomas (HCC) are malignant tumors that primarily affects hepatocytes, the main cells of the liver. While uncommon, they can occur in all domestic species. They are more frequent in cattle and dogs, while quite rare in cats, sheep, pigs and horses [28, 48, 49]. HCC is however more frequent in humans with hepatitis B, hepatitis C and cirrhosis being the main risk factors [50, 51]. For that reason, various studies on hepatocellular carcinoma have been conducted using laboratory rats as models. These mostly involve the administration of carcinogens or genetic manipulations to induce tumor formation in the rat

liver [52]. To the best of our knowledge, there is no report of spontaneous hepatocellular carcinoma in pet rats.

2.3.1.2. Clinical apperance

Hepatocellular carcinoma in domestic species might manifest with non-specific clinical signs including anorexia, lethargy, ascites and vomiting and less commonly, icterus, diarrhea and weight loss. In cats with HCC, alepecia has also been reported but is not frequent.

Biochemistry is often not specific, with possible mild elevation of liver enzymes. Horses and dogs with HCC might present hypoglycemia and subconsequent seizures. Diagnostic methods include measurement of serum α-fetoprotein as a non-specific HCC marker, diagnostic imaging and ultrasound-guided fine needle aspiration or biopsy with histopathological analysis [49].

2.3.1.3. Gross morphology

Hepatocellular carcinomas most often present as single neoplasm involving one liver lobe, but tend to replace most of the normal liver tissue within this lobe. HCC can be found in any liver lobes, but it seems that the left liver lobes (left lateral, medial lobes and papillary process of the caudate lobe) are most frequently affected in dogs [53]. In particular, the left lateral liver lobe is a frequent site for HCC, which could be related to its more important mass [49].

Their apperance can vary between massive (Figure 7A), nodular (Figure 7B), and diffuse forms, with massive being the most commonly observed form in cattle and dogs [49]. Small neoplasms are likely to be uniform and resemble normal liver, while larger masses typically consist of friable, gray-white or yellow-brown tumors, respectively due to extensive necrotic areas and lipodosis [28, 48, 54]. The soft apperance of HCC can help differentiating them from cholangiosarcoma, which have a firmer consistency [49].

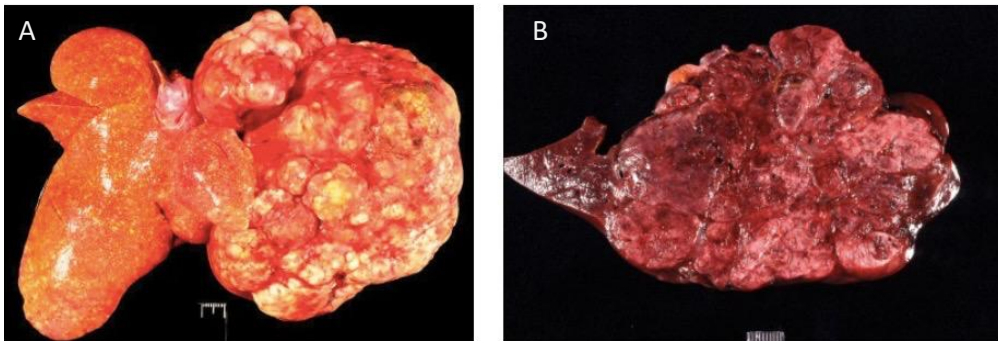

Figure 7: Gross appearance of hepatocellular carcinoma (Meuten, 2002)
A: Massive form of HCC in a cat. B: Nodular form of HCC in a dog.

2.3.1.4. Histological features

The histological appearance of hepatocellular carcinomas can vary greatly, depending on the degree of differentiation of the tumorous hepatocytes and their cellular arrangement. However, three major histological patterns can be identified: trabecular, solid and pseudoglandular. In domestic animals, scirrhous and clear cell type also exist but remain very uncommon [28, 48, 49, 54, 55].

In trabecular HCC, the neoplastic hepatocytes tend to form irregular thick plates composed of three or more cells, called trabeculae (Figure 8). Those trabeculae vary in thickness within the tumorous tissue: they can be quite thin (maximum five cells) in some sites and markedly thick (more than ten cells) in other sites [49]. The trabeculae are often separated by large sinusoidal spaces, which may be filled with erythrocytes (Figure 8) [28, 48]. In the center of wide trabeculae, necrosis can occur [49].

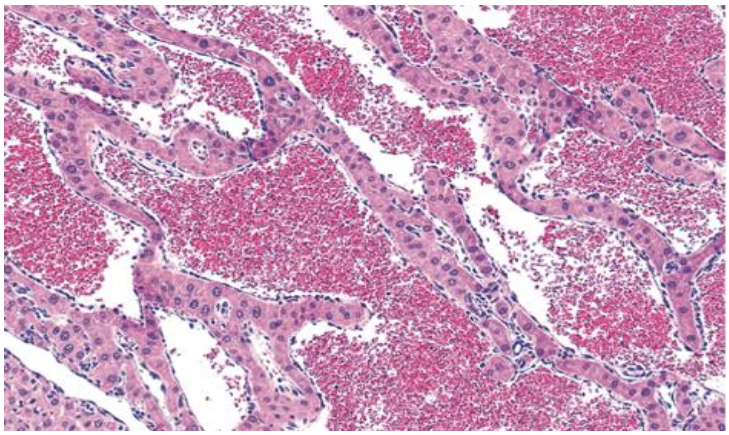

Figure 8: Trabecular hepatocellular carcinoma (dog, Barthold et al., 2016)
The hepatocytes form plates or trabeculae. The sinusoids contain erythrocytes.

In solid HCC, sheets of neoplastic hepatocytes are arranged without apparent pattern, lacking sinusoids and appearing like a solid block of cells (Figure 9) [49].

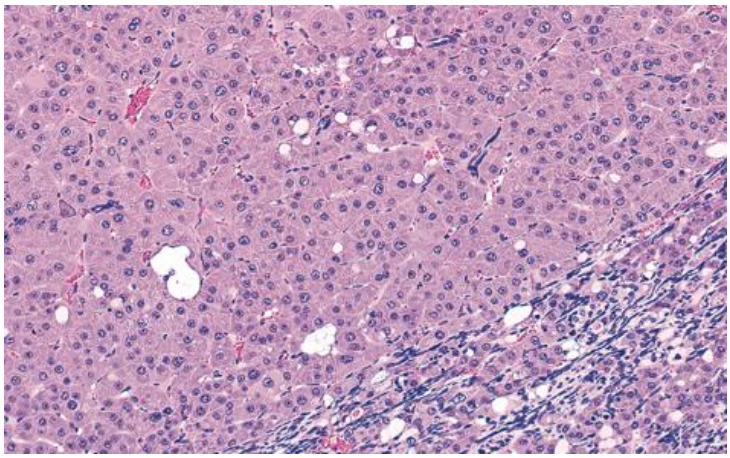

Figure 9: Solid hepatocellular carcinoma (Barthold et al., 2016)
The hepatocytes are in close proximity without particular pattern and compress normal tissue (lower right corner). The sinusoids are barely visible.

The pseudoglandular HCC is characterized by formation of acini, which may be filled with a protein-rich content resembling a glandular arrangement (Figure 10) [28, 48, 49, 56]. Those acini however never contain mucous, which can help differentiating them from cholangiocarcinoma [49].

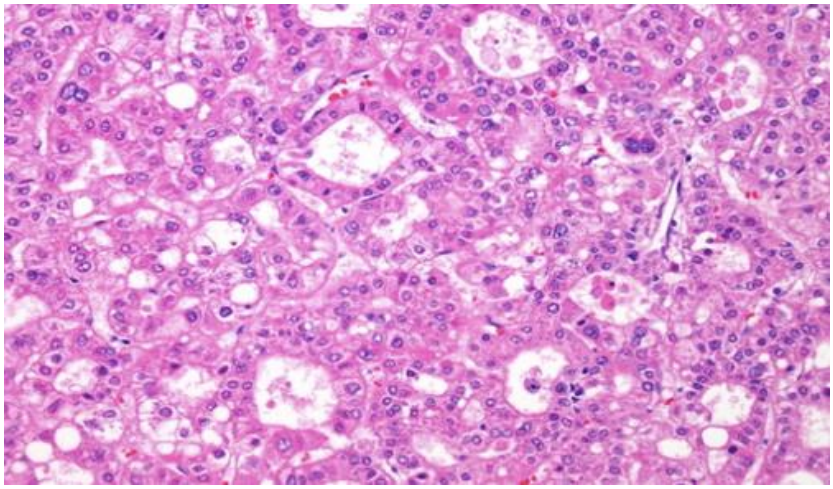

Figure 10: Pseudoglandular hepatocellular carcinoma (human, webpathology.com)
The hepatocytes are arranged in acini.

In domestic animals, the scirrhous HCC is very uncommon but consists of dense connective tissue embedding a ductular structures surrounded by neoplastic hepatocytes (Figure 11). Those duct-like structures can be stained for cytokeratin using immunochemistry [49].

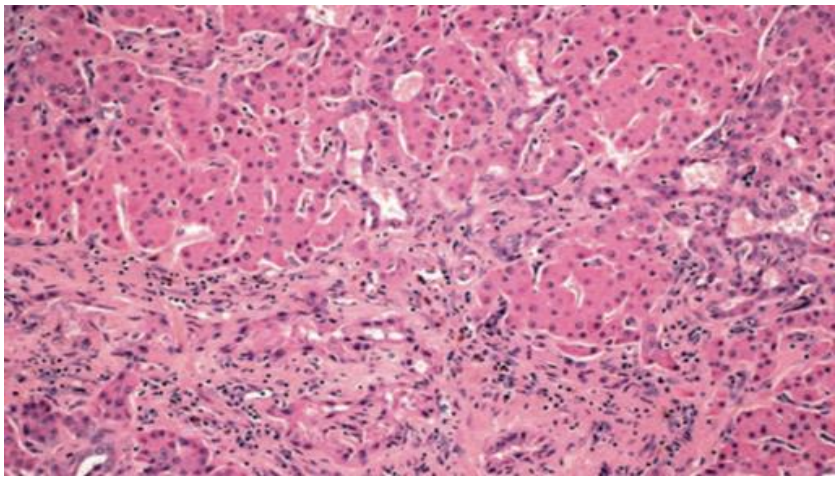

Figure 11: Scirrhous hepatocellular carcinoma (dog)
A: Solid hepatocellular lower magnification (Zachary, 2017). B: Solid hepatocellular higher magnification (Meuten, 2002). The hepatocytes surround ductular structures. Note the high amount of connective tissue.

Clear cells HCC are composed of vacuolised hepatocytes with high glycogen and lipid content (Figure 12) [49].

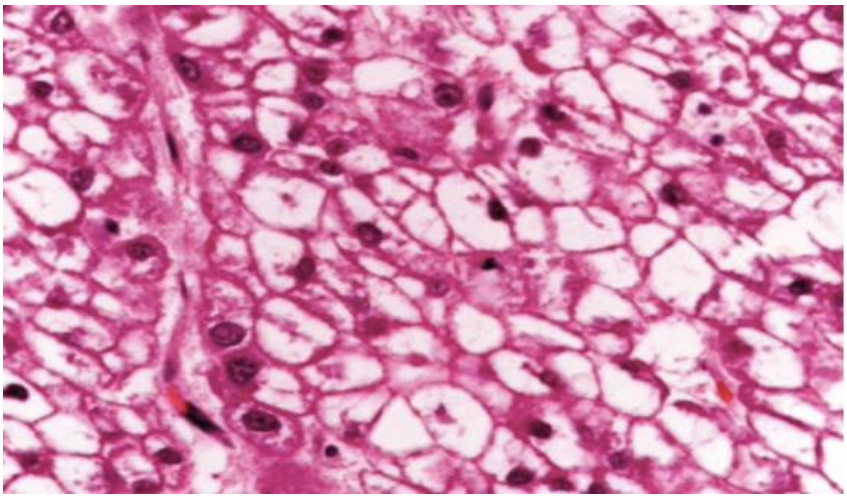

Figure 12: Clear cell hepatocellular carcinoma (dog, Meuten, 2002)

The cellular appearance of the neoplastic hepatocytes can range from well-differentiated cells to atypical (*atypia*) [28].

When well-differentiated, they resemble normal hepatocytes with a central round nuclei and a moderaly eosinophilic cytoplasm which can appear paler if glycogen or lipid accumulate in it. In trabecular and pseudoglandular HCC hepatocytes are mostly moderately to well-differentiated (Table 1) [57].

Poorly differentiated HCC are composed of pleomorphic hepatocytes with variable size and shape, more basophilic cytoplasm, and can include giant cells [48, 49]. In particular, pleomorphic and multinucleated giant cells are typical in solid HCC. The neoplastic cells usually lacks the polygonal shape of normal hepatocytes and may appear round or rarely spindle-shaped. Their nuclei tend to be enlarged and of different sizes. Solid HCC are mostly composed of poorly differentiated hepatocytes [57].

Table 1: Cellular characterization of hepatocellular carcinoma (Gisder et al., 2022)

Grades	Architecture	Cytology	Other features
Well differentiated	Thin trabecular, frequent acinar structures	Minimal atypia	Fatty change is frequent
Moderately differentiated	Trabecular (more than 3 cells thick) and acinar	Abundant eosinophilic cytoplasm, round nuclei with distinct nucleoli	Bile or proteinaceous fluid with acini
Poorly differentiated	Solid	Moderate to marker pleomorphism	Absence of sinusoid-like blood spaces
Undifferentiated	Solid	Little cytoplasm, sindle or round-shaped cells	-

Vascular invasion is typical in HCC and spreading might extend to the hepatic veins and *vena cava* [48]. Portal areas are also most often not recognisable [54].

2.3.1.5. Metastasis

In hepatocellular carcinoma of domestic animals, metastasis is uncommon [28, 48]. The metastatic rate varies from 0% to 37% for dogs with massive HCCs and 93% to 100% for dogs with nodular and diffuse HCCs [53]. When present, metastases can be either intrahepatic to one or several liver lobes, or extrahepatic via hematogenous or lymphogenous spreading. In dogs, distant metastasis is rare but may occur in sites such as the regional lymph nodes of the cranial abdomen, the lungs (Figure 13) and the peritoneum [48, 53]. Other metastatic sites include the heart, kidneys, adrenal glands, pancreas, intestines, spleen, and urinary bladder [53].

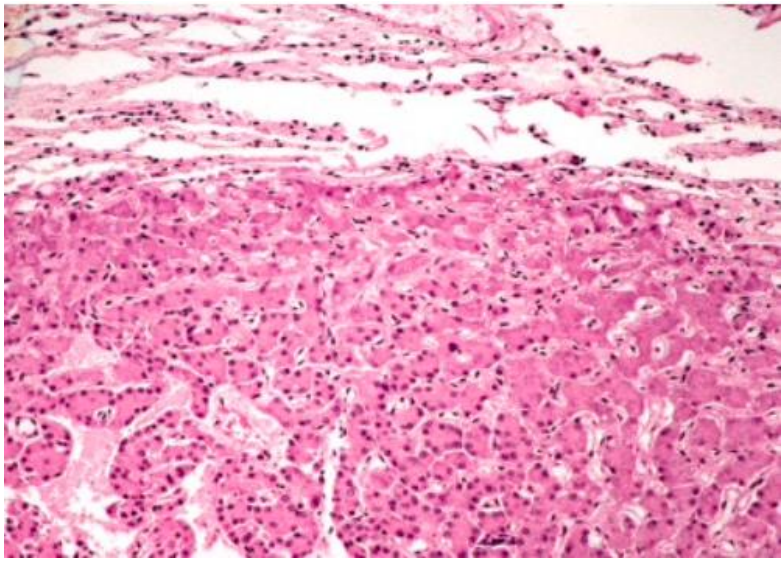

Figure 13: Pulmonary metastasis in a dog with hepatocellular carcinoma (Meuten, 2002).

2.3.1.6. Staging and grading

Hepatocellular carcinoma being relatively rare in domestic animals, HCC grading systems are adapted from human medicine literature. HCC can be staged using the TNM classtification system, evaluating malignancy [58] (Table 2).

Table 2: TNM staging system of dog hepatocellular carcinoma (Marcanato et al., 2020)

Primary tumor (T)	T0: no evidence of primary tumor T1: solitary tumor of any size involving one lobe T2: multiple tumors of any size involving multiple lobes T3: tumor(s) with direct invasion of adjacent organs
Regional lymph nodes (N)	N0: no regional lymph nodes metastasis N1: regional lymph node metastasis N2: distant lymph node metastasis
Distant metastasis (M)	M0: no distant metastasis M1: distant metastasis

Histological grading of HCC is based on the nuclei, nucleoli and architecture of the tumor [59, 60] (Table 3).

Table 3: Histological grading of hepatocellular carcinoma (Martins-Filho et al., 2017)

Grade	Nuclei	Nucleoli	Architecture
I	Homogenous, near-normal nuclei	Nucleoli barely seen at 400x	Trabecular, 2-3 cell wide
II	Mild pleomorphism	Evident nucleoli at 100-200x	Pseudoglandular pattern
III	Moderate pleomorphism, irregular distribution of chromatin	Large nucleoli visible at 100x	Mild trabecular (4-10 cells wide)
IV	Marked pleomorphism, bizarre nuclei	Prominent nucleoli visible at 40x	Macro-trabecular (>10 cells wide) or solid bizarre pattern

2.3.1.7. Prognosis

The prognosis for massive hepatocellular carcinomas (HCC) is good, as complete surgical resection is possible and their behavior is relatively non-aggressive. In contrast, the prognosis for cats and dogs with nodular and diffuse liver tumors is poorer, because metastasis is more common [53].

2.3.1.8. Differential diagnosis

The most challenging differential diagnosis of well-differentiated HCC is the hepatocellular adenoma. Extrahepatic metastasis and cellular invasion into adjacent healthy tissue or into the vessels are key criteria to establish malignancy. However, those features are not always present in HCC. Other useful features of malignancy include pleomorphic hepatocytes, atypical or multinucleate hepatocytes, mitotic figures, multiple nucleated cells, absence of clear demarcation and trabeculae of variable thickness [48, 49].

Pseudoglandular HCC can be difficult to differentiate from cholangiocarcinomas. In both cases, neoplastic acini can be observed. While HCC acini may be full of proteineaceous material and never mucus, mucin content can be found in cholangiocarcinomas. Hence, Peridic Acid Staining staining is more likely to be positive in cholangiocarcinomas and can be used for differentiation [49].

Immunohistochemistry is a useful tool to identify HCC and distinguish them from other neoplasms. Identification of a most cats and dogs HCC involves the use of the Hepatocyte Paraffin 1 or HepPar-1 staining. This staining recognizes mitochondrial antigen of hepatocytes, using monoclonal antibodies [48, 49, 61] and is used to differentiate HCC from cholangiocarcinoma or metastases to the liver [61–63]. However, it is worth noting that in

some poorly differentiated HCC, the cells aggregate and no longer stain with HePar1, and the use of staining of cytokeratin 19 might be recommended, as it identifies hepatocytes progenitor cells [49].

2.3.2. Stellate cell hyperplasia and tumors

Hepatic stellate cells (HSC) hyperplasia is abnormal proliferation of activated HSC and is associated with liver damage and inflammation. In rodents, it is often seen in *Helicobacter* infection, but numerous other diseases can cause this condition. Activated HSC exhibit proinflammatory, profibrogenic and promitotic properties. Therefore, marked increase in inflammatory cells, mostly lymphocytes and plasma cells, as well as collagen accumulation is associated with HSC hyperplasia [64].

HSC tumors are very rare in humans and in animals. In general, mesenchymal tumors of the liver are very rare and HSC tumors even rarer, making scientific literature quite scarce. In most cases, mesenchymal tumors are diagnosed and stellate cell tumor only suspected, due to the difficulty to confirm them [64].

HSC tumors are more common in mice than other animals [55, 64] and are described as moderately firm, due to the fibrous stroma and increased collagen content infiltrating between hepatocytes and around tumor. Tumorous stellate cells vary from round and vacuolated to spindle shaped with elliptical nucleus. These cells often interconnect with each other, forming a reticular structure.

3. Materials and methods

3.1. Clinical presentation

A 15 month-old non-castrated male dwarf pet rat was presented to the exotic clinic of the University of Veterinary Medicine Budapest (UVMB) for a penile prolapse associated with lethargy and dyspnea. The animal was also hypothermic, dehydrated and his coat was unkept. An adhesive tape hair sampling was performed. Auscultation of the lungs confirmed increased respiratory sounds and moderate to severe dyspnea (Figure 14A). The nostrils were clear of any discharge. Physical palpation revealed a non-movable nodular mass in the left ventral abdominal wall. After manual retractation of the penis into the prepuce, the rat received fluid therapy (6mL of Duphalyte infusion subcutaneously) and was placed in an oxygen cage for stabilization. The microscopic examination of the fur revealed numerous empty lice nits, suggesting lice infestation (Figure 14B). The rat was treated with Ivermectin (0.05mL Ivermectin 1% subcutaneously). Despite 3h of oxygen therapy, the rat's condition worsened and he was euthanised upon request of the owner.

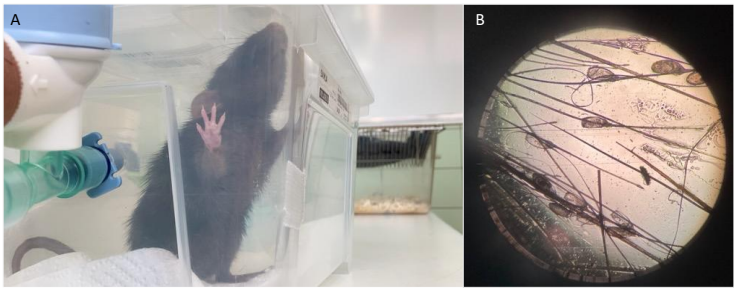

Figure 14: Clinical presentation of the patient
A: Relieving posture of the patient due to dyspnea. B: Empty lice nits (optic microscope, 100x)

3.2. Tumor collection

A rapid necropsy was performed, by the wish of the owner, at the UVMB exotic clinic. Numerous masses were found in the abdominal and thorassic cavity, on the liver, common bile duct and lung. Out of them 4 masses were excised and fixed with 10% neutral-buffered formalin solution at room temperature for 24h.

One 12 mm mass was removed from the LLL with some healthy-looking liver tissue. One mass (10 mm) was excised from the common bile duct. Two other masses (4 and 6 mm) from the lungs were excised with a portion of healthy lungs (accessory lobe).

3.3. Histopathology

Histopathological analysis was performed by Pr. Balka, associate professor from the Department of Pathology of the UVMB. Excised tumors were embedded into a paraffin block and sections of 3–4 µm were performed using a microtome. Sections were then either stained with H&E, Hepatocyte Paraffin 1 (HepPar-1), α-smooth muscle actin (α-SMA), Claudin-5 and factor VIII staining (Table 4).

Table 4: Histopathological staining used in the study

Staning	Marker of	Positive staining associated processes and diseases
HepPar-1	Hepatocytes michondria	▪ Processes of hepatocellular origin [65] ▪ Hepatocellular carcinoma (differentiation with cholangiocarcinoma and liver metastasis) [61, 65]
α-SMA	Smooth muscles, myofibroblasts	▪ Activation of myofibroblasts [66, 67] ▪ Epithelial mesenchymal transition of carcinomas [66]
Claudin-5	Endothelial tight junctions	▪ Angiosarcoma or hemangioendothelioma [68, 69] ▪ Pancreatic solid papillary neoplasm [69, 70] ▪ Other carcinomas
Factor VIII	Endothelial cells	▪ Vascular tumors [71]

The slides were scanned, and representative images were taken (Pannoramic Midi II slide scanner; Case-Viewer and QuPath softwares; Budapest, Hungary). Tumor type evaluation and description were performed with the help of Dr. Szilasi, senior lecturer and Pr. Mándoki, professor and head of the Pathology department at UVMB.

4. Results

4.1. Left liver lobe mass

4.1.1. Gross appearance

The excised mass at the apex of the left lateral lobe was round, lobulated in appearance, measuring approximately 8-10 mm in diameter. Its color was pale pink, it had soft consistency and a smooth surface, with margins looking well defined. The mass was observable on both the diaphragmatic and the viceral sides of the liver, appearing as it emerged from the liver parenchyma. Vasculature was prominent and two smaller satelite masses were visible close to the main mass (Figure 15). No cross-section was made prior to fixation. The surrounding liver tissue appeared healthy, without macroscopic evidence of fibrosis or inflammation.

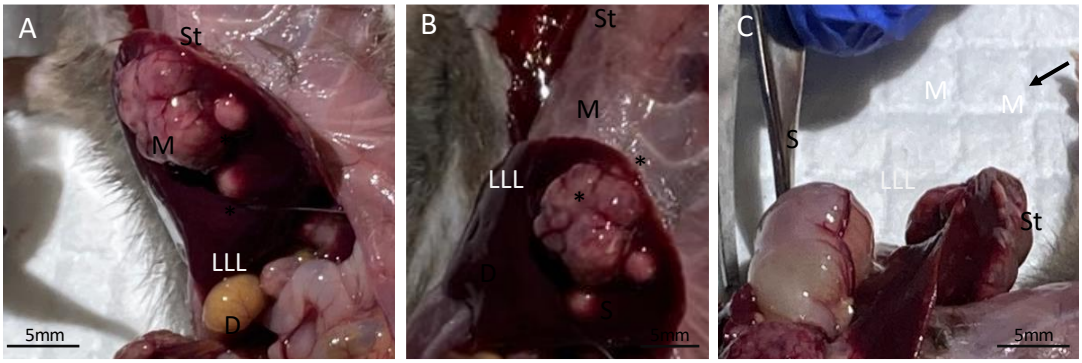

Figure 15: Gross appearance of the left liver lobe tumor. A, B: Ventral views showing the visceral surface. C: Lateral view showing both visceral and diaphragmatic surfaces.
D: duodenum, LLL: left liver lobe, M: mass, *: satellite masses, St: sternum, S: stomach, arrow: diaphragmatic surface

4.1.2. Histological features

The left liver lobe parenchyma was occupied and expanded by a lobulated, large (approximately 12 mm long axis and 9 mm short axis), densely cellular and well-demarcated, however unencapsulated mass. The cells in the parenchyma of the mass were arranged in non-structural clusters which were more basophilic compared to the tissue of the healthy liver portion (Figure 16). Broad, eosinophilic network of cellular stroma infiltrated between the clusters, supporting the mass. The mass itself was very well vascularized with numerous large blood vessels, except for its avascular center (Figure 17). The center of the mass was pale pink in appearance where cells with bright eosinophilic cytoplasm showed sign of karyopyknosis, karyolysis and karyorrhexis, indicative of necrosis. The necrotic center was surrounded by stroma (Figure 17).

Figure 16: Left liver lobe mass, low magnification (H&E, 14x)
1: necrotic center, 2: blood vessels, 3: healthy liver tissue, 4: more basophilic lesion

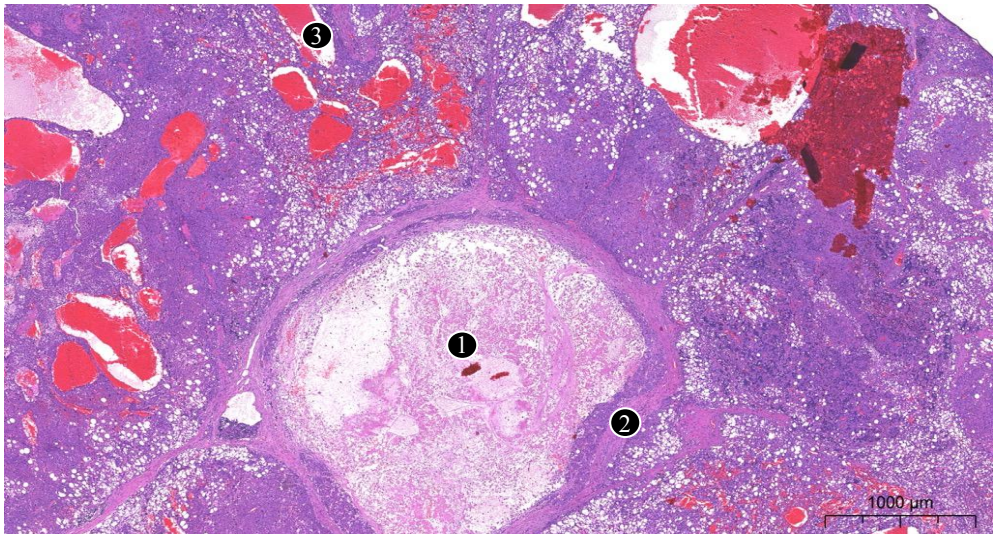

Figure 17: Left liver lobe mass, necrotic center (H&E, 32x)
1: necrotic center, 2: stroma, 3: blood vessel

The cells in the clusters were variable in both shape and size. Cells were polygonal, rounded or elongated due to compression. Some cells were relatively large with a lot of cytoplasm while others contained very little and were hardly bigger than their nuclei (Figure 18).

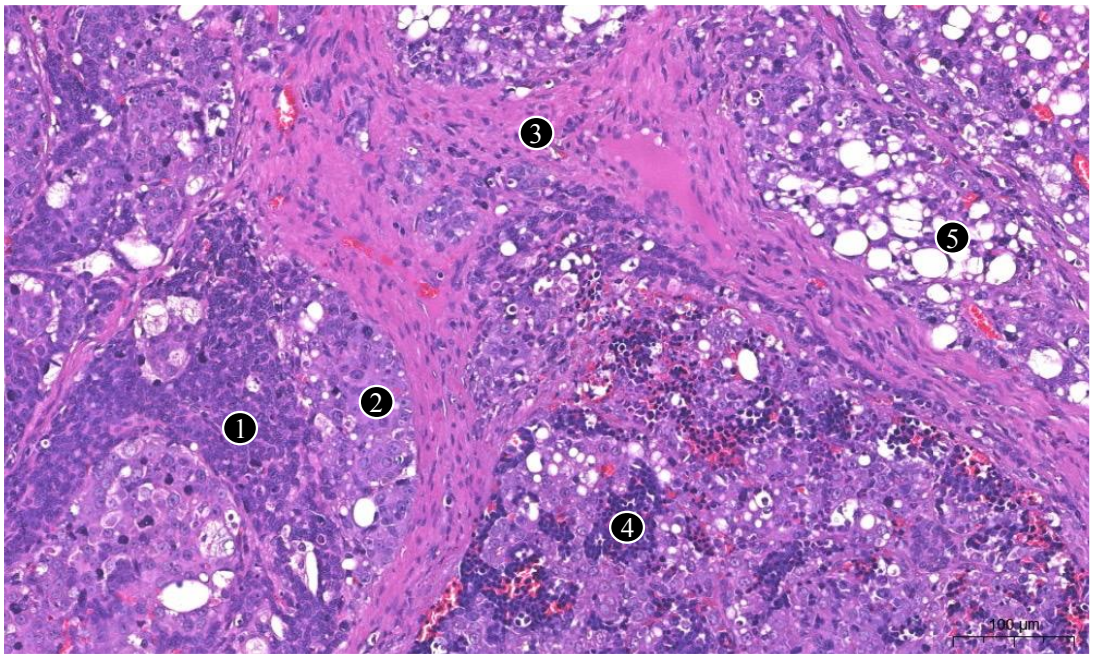

Figure 18: Left liver lobe mass, cellular pleomorphism (H&E, 280x)
1: poorly differentiated cells, 2: moderately differentiated cells, 3: stroma, 4: lymphocytes, 5: vacuolated cells. 1, 2, 3 illustrate cellular pleomorphism within the neoplasm.

Their cytoplasm was stained purple, showing both eosinophilic and basophilic characteristics. Vacuoles of varying size could be found in some cells, with some of them covering the whole cytoplasm. The margins of the cells were frequently not clearly defined especially in the cells showing more basophilic staining. The nuclei were typically round or oval, large and mostly centrally located. In the large vacuolated cells, the nuclei had been pushed towards the periphery. The chromatin appeared often granulated but in some of the smaller cells it was both more uniform and more intensely stained. The nucleolus was quite prominent and often double. There was marked anisokaryosis and anisocytosis. Occasional multinucleated cells were spotted (Figure 19). Numerous mitotic figures were seen per, some with unusual appearance, suggestive of tumorous process (Figure 20). Clusters of lymphoid cells with dark round basophilic nucleus could be seen scattered around the mass (Figure 18). Several times, clusters of neoplastic cells were present within blood vessels, suggestive of vascular invasion (Figure 21). The mass margins were distinguishably separated from the liver parenchyma and the healthy liver parenchyma next to the tumor looked compressed.

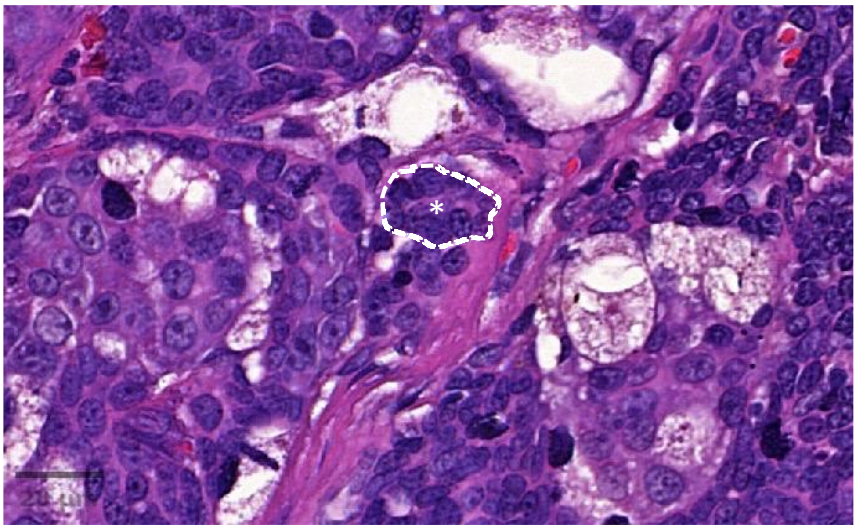

Figure 19: Left liver lobe mass, multinucleated cell (H&E, 900x)
The dotted line marks the borders of a multinucleated cell.

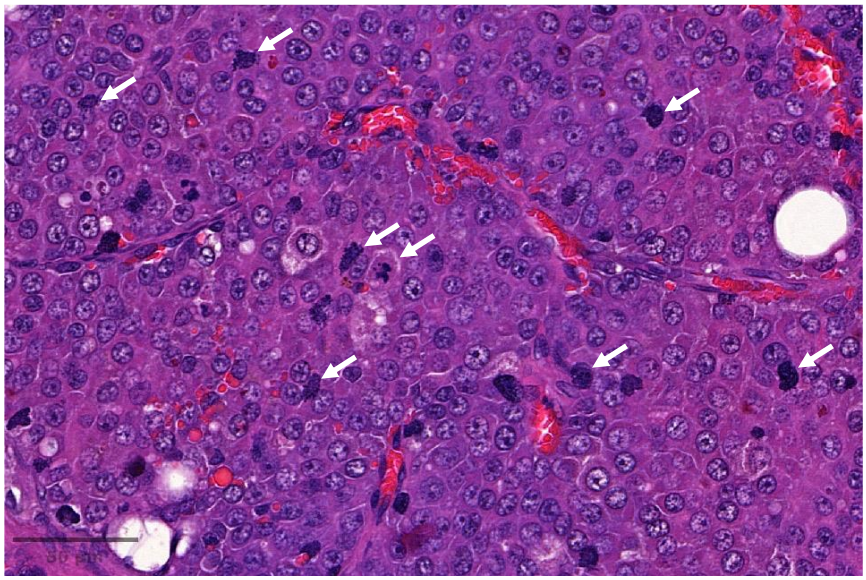

Figure 20: Left liver lobe mass (H&E, 560x)
The white arrows indicate mitotic figures.

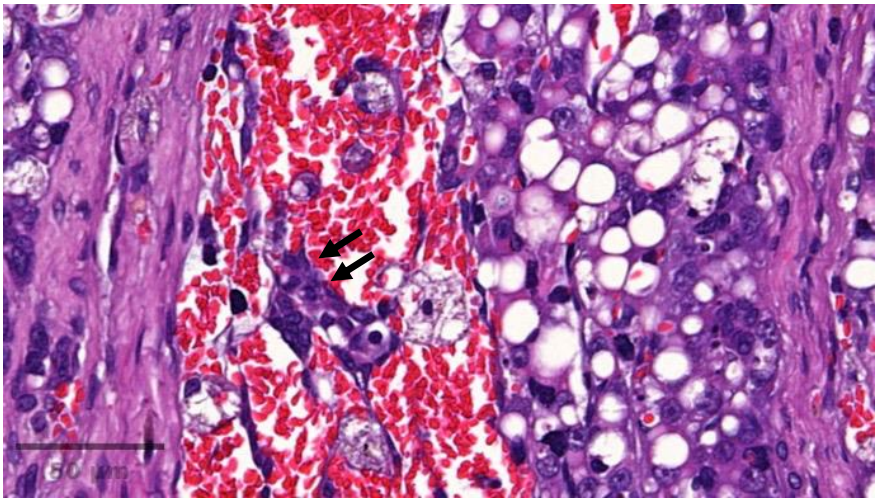

Figure 21: Left liver lobe mass, vascular invasion (H&E, 580x)
The black arrows point at parenchymal cells occupying the lumen of a blood vessel.

The mass was claudin-5 and Factor VII negative but HepPar-1 positive, suggesting hepatocyte originated cells. The cellular clusters between the stroma of the mass itself displayed uneven sporadic staining where the cytoplasm appeared granulated (Figure 22). HepPar-1 positive cells were also found within the vasculature of the liver mass (Figure 23). Comparatively, the healthy liver area stained rather uniformly with HepPar-1, nicely displaying the hepatic lobule-hepatic plate arrangement, lost in the mass (Figure 24).

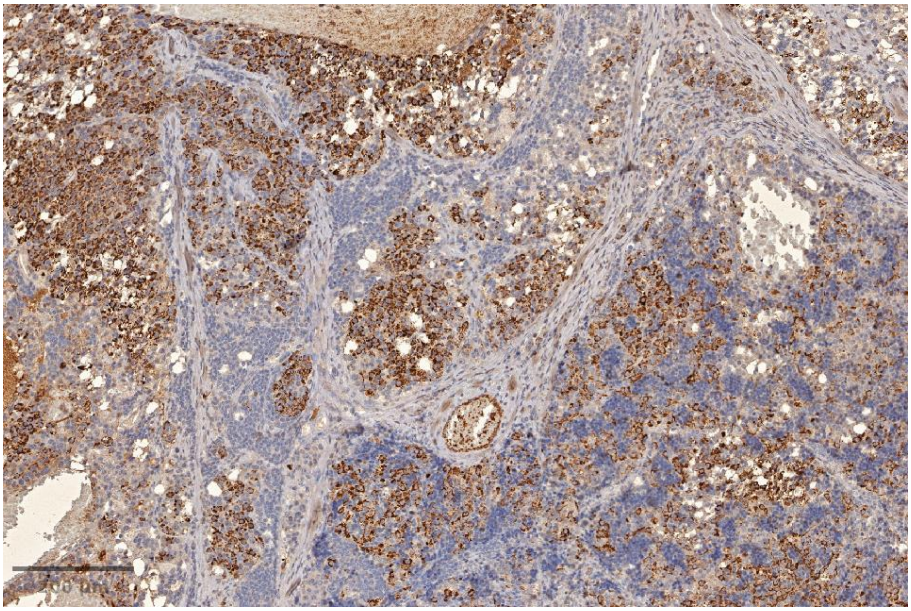

Figure 22: Left liver lobe mass, patchy staining of the parenchyma (HepPar-1, 160x)

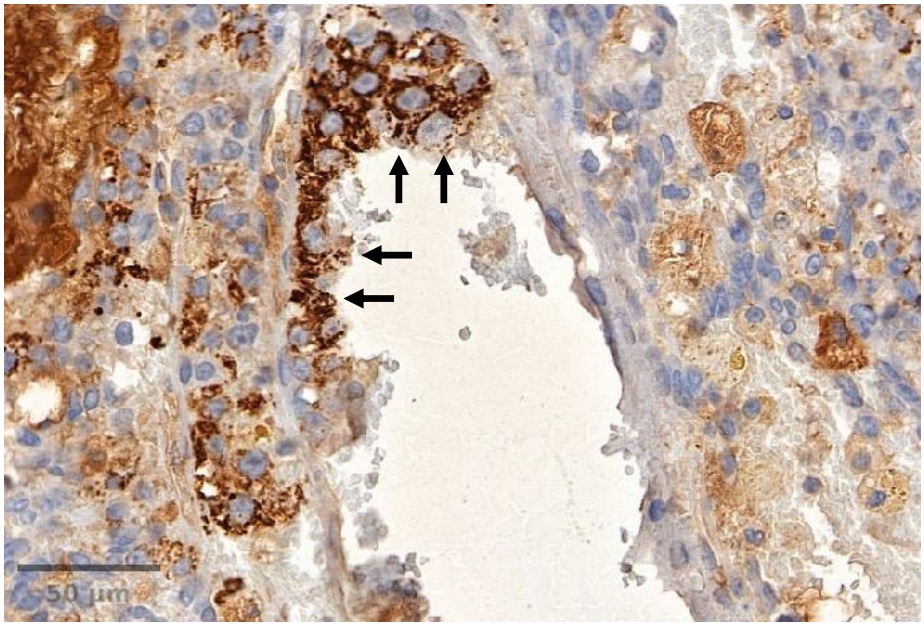

Figure 23: Left liver lobe mass, blood vessel invasion (HepPar-1, 540x)
The arrows point at HepPar-1 positive cells invading a blood vessel.

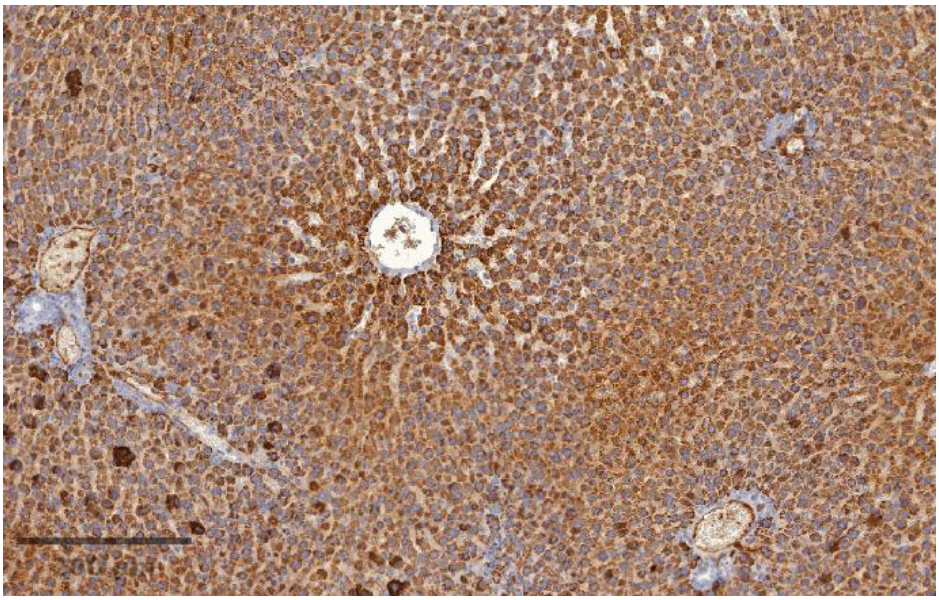

Figure 24: Left liver lobe, healthy hepatic lobule with uniform staining (HepPar-1, 160x)

The stroma of the mass was positive for α-SMA staining and showed intense staining, nicely displaying septa within the mass. Within the mass parenchyma, some cellular clusters displayed α-SMA positive extensions (Figure 25) likely associated with the presence of myofibroblast-like cells, while other clusters were mostly negative (Figure 26). On the other hand, the healthy liver segment was mostly negative (Figure 27), except for the portion of the liver near the margin of the mass (Figure 28).

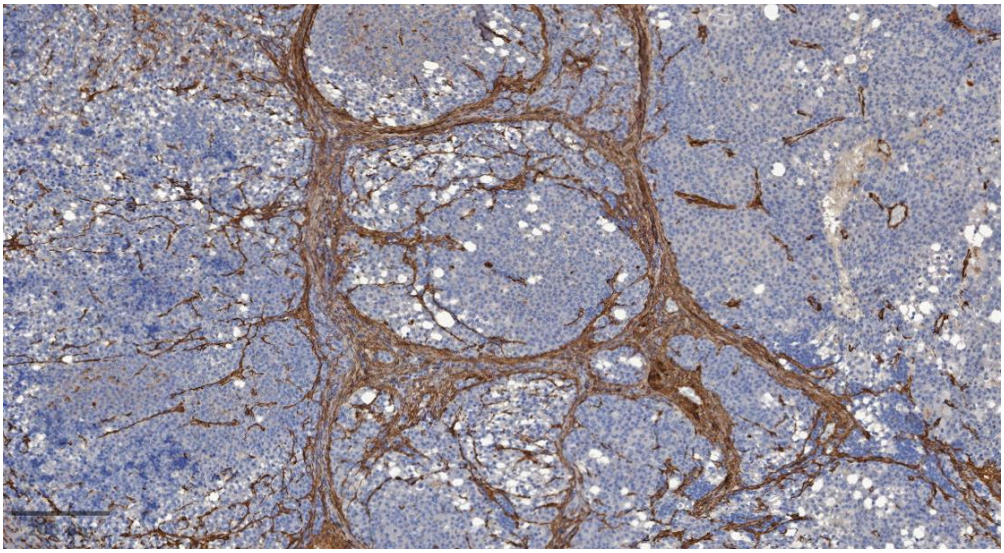

Figure 25: Left liver lobe mass, α-SMA positive stroma and parenchymal cell clusters (α-SMA, 120x)

Note the intensively stained stroma and the stained branches running in between the cells of the liver mass' parenchyma.

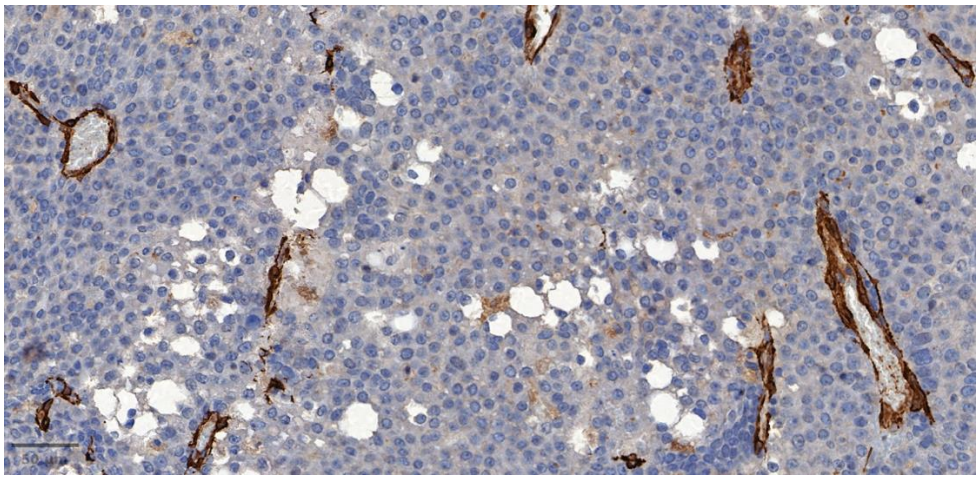

Figure 26: Left liver lobe mass, negative α-SMA clusters (α-SMA, 400x).
The positive α-SMA areas are blood vessels.

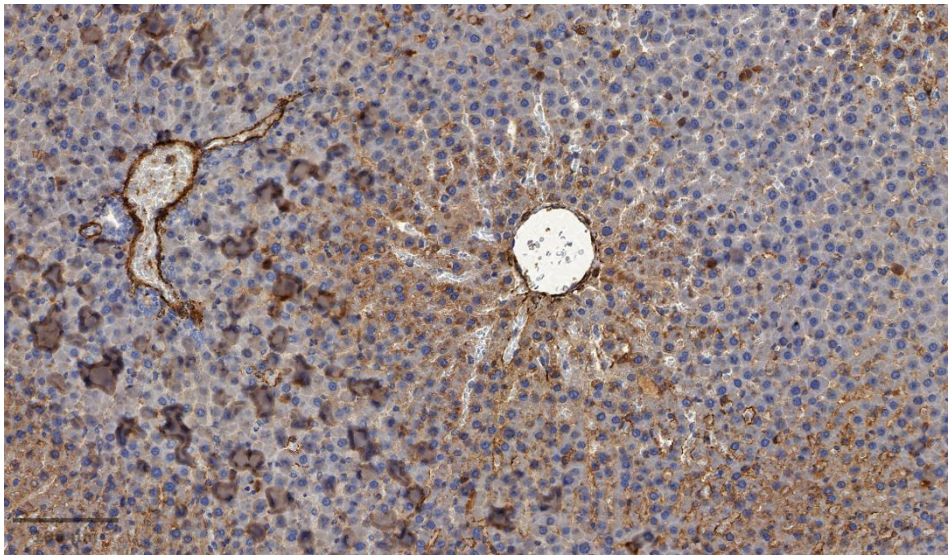

Figure 27: Left liver lobe, negative α-SMA staining around healthy liver lobule (α-SMA, 280x).
The α-SMA stained structures are blood vessels.

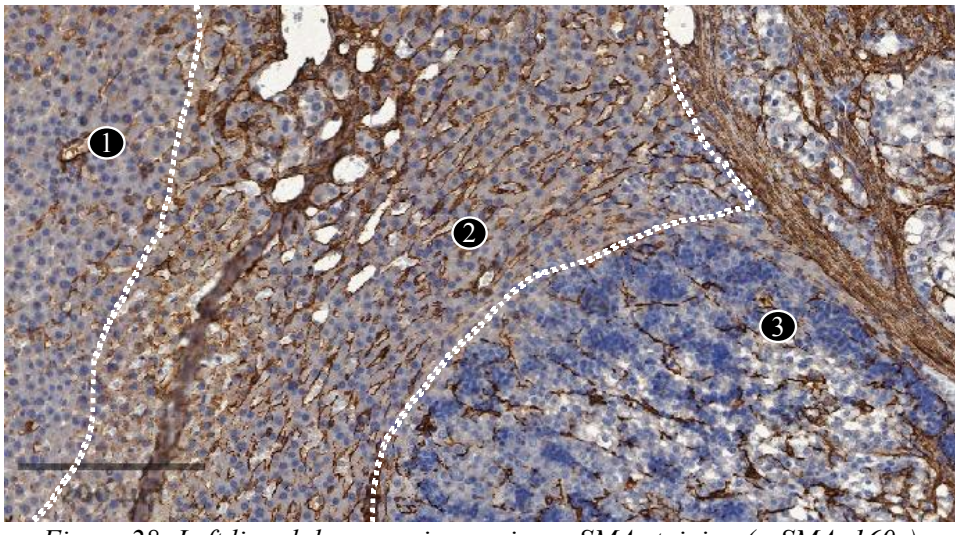

Figure 28: Left liver lobe mass, increasing α-SMA staining (α-SMA, 160x)
1: healthy liver parenchyma with negative α-SMA staining, 2: compressed tumoral zone with moderate α-SMA staining, 3: tumoral zone with intense α-SMA staining.

4.2. Bile duct mass

4.2.1. Gross appearance

A pendulus bean shaped mass of approximately 10 mm in length was attached to the common bile duct (*choleductus*). Its colour was pale pink, spotted with yellow discolourations due to bile imbibition (Figure 29A, B). Its appeared lobulated with a soft consistency. On the surface, the vasculature was prominent and the cut surface revealed central necrosis (Figure 29C).

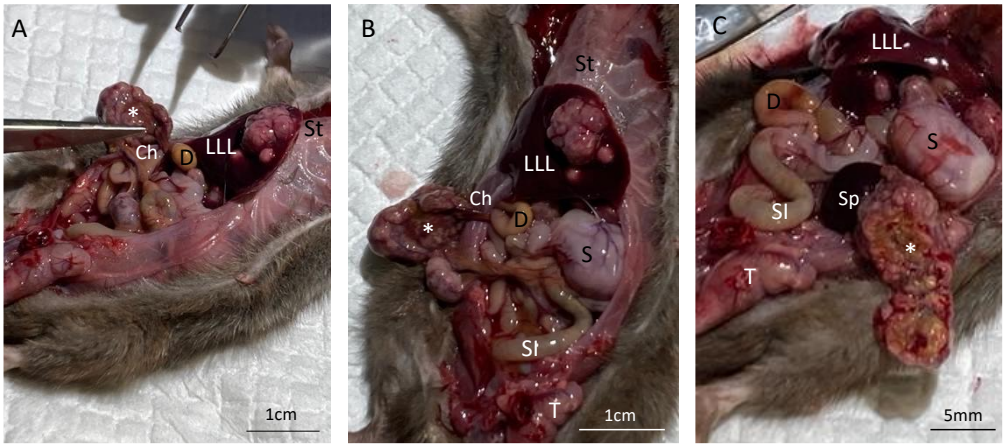

Figure 29: Gross appearance of the bile duct mass.
*: mass, Ch: choleductus (bile duct), D: duodenum, LLL: left lateral lobe, S: stomach, SI: small intestines, Sp: spleen, St: sternum, T: testis.

4.2.2. Histological features

The shape of the excised mass was difficult to describe due formation of gaps in the section. The mass was densely cellular, well-demarcated, well-vascularized and encapsulated, with a thick capsule (Figure 30).

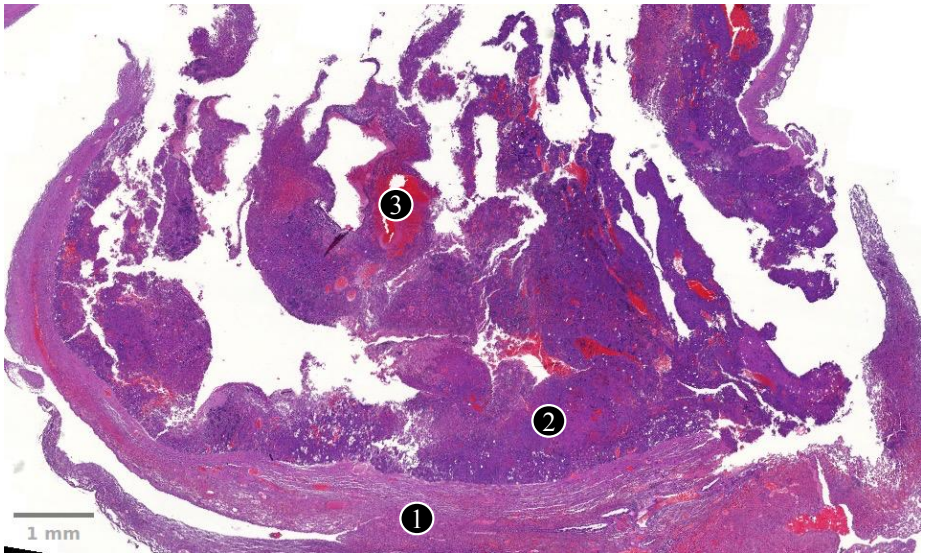

Figure 30: Bile duct mass, low magnification (H&E, 21x)
1: capsule, 2: parenchyma, 3: one blood vessel

The cells in the parenchyma were arranged in clusters forming solid aggregates. Density within the clusters varied from moderately dense with recognisable structural arrangement to more densely packed and dysorganised. The cells in the more organised areas had pink cytoplasm and resembled hepatocytes but lobular arrangement could not be identified. The cells within the dense aggregates appeared purple with more basophilic cytoplasm, looking less differentiated (Figure 31). Vacuolated cells could be found at the periphery of the mass, but were fewer compared to the left liver lobe mass (see 4.1.2). The margins of the parenchymal cells were variably defined, with the solid aggregates being poorly defined, but increased structual arrangement resulted in better defined margins (Figure 31).

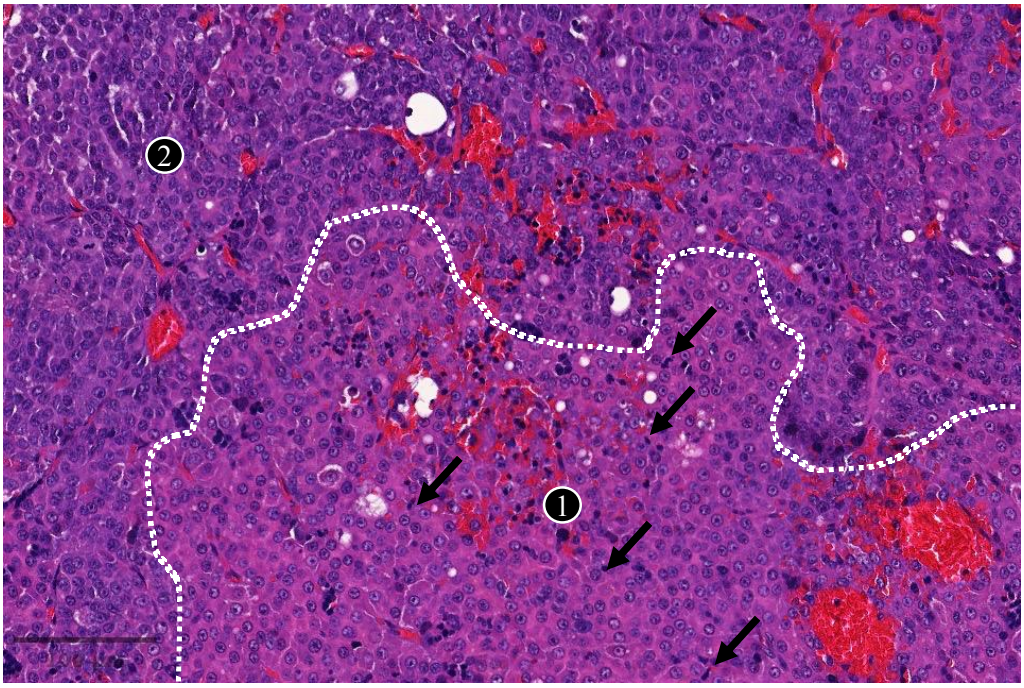

Figure 31: Bile duct mass, cellular morphology (H&E, 350x)
1: moderately dense eosinophilic cells with more defined margins, 2: dense basophilic aggregates. Arrows: mitotic figures

The nuclei of the parenchymal cells were typically round or oval, large and mostly centrally located. They had basophilic granulated to solid looking chromatin with one or two nucleoli. Marked anisokaryosis and anisocytosis was present, especially in the solid aggregates (Figure 31). Lymphoid cells with dark round basophilic nucleus could be seen scattered throughout the mass.

A pale pink area contained degenerative cells showing sign of karyopyknosis and karyolysis, suggestive of necrosis. This area was not surrounded by stroma (Figure 32), unlike the the necrotic center of the liver mass (see 4.1.2).

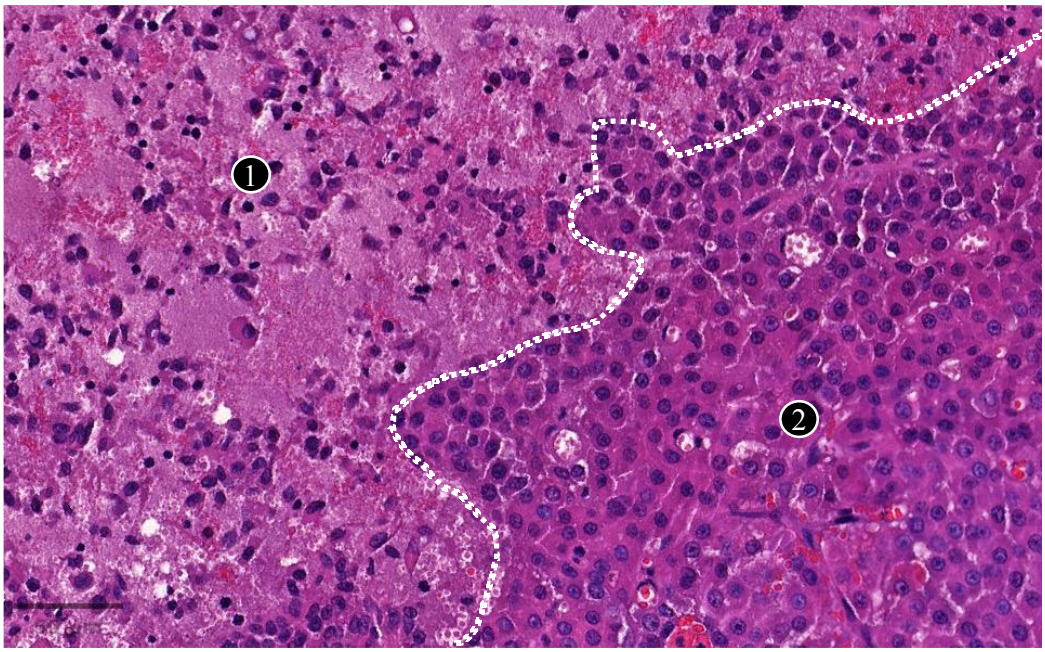

Figure 32: Bile duct mass, necrotic area (H&E, 500x)
1: necrotic area, 2: mass parenchyma

The capsule of the mass was formed of eosinophilic, spindle shaped cells with elongated nucleus, and fibers resembling collagen.

The bile duct mass presented negative Claudin-5 and Factor VII stainings. HepPar-1 was however positive with scattered appearance (Figure 33).

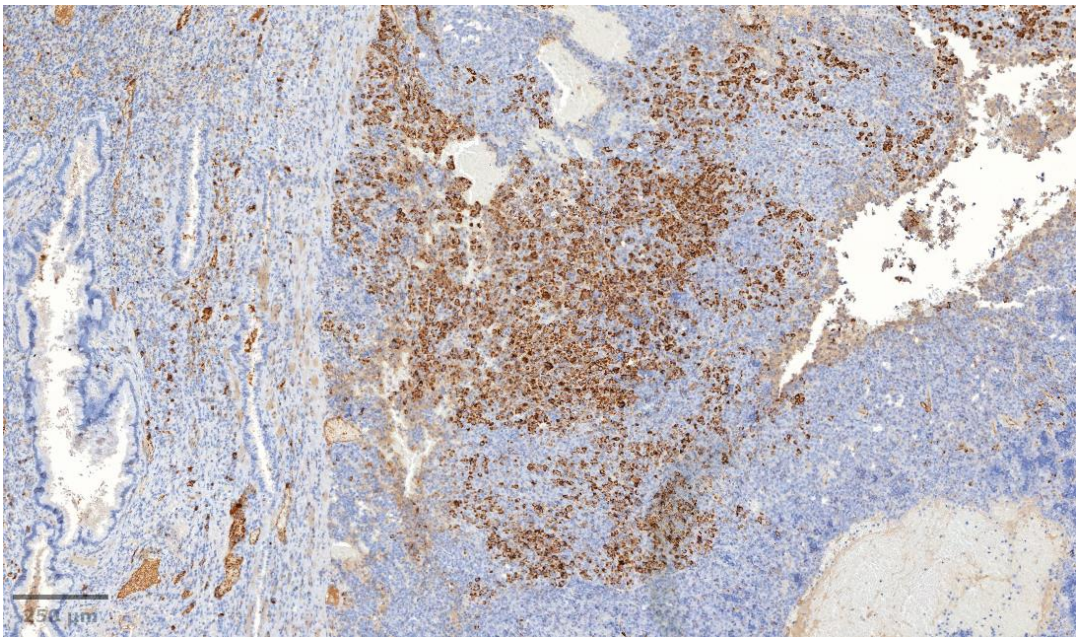

Figure 33: Bile duct mass, patchy appearance HepPar-1 staining in the mass parenchyma (HepPar-1, 80x)

The capsule of the mass stained positive for α-SMA and included spindle shaped cells. Within the mass, α-SMA positive branching cells were present (Figure 34). Mitotic figures were found but to lesser extent compared to the left liver lobe mass (see 4.1.2).

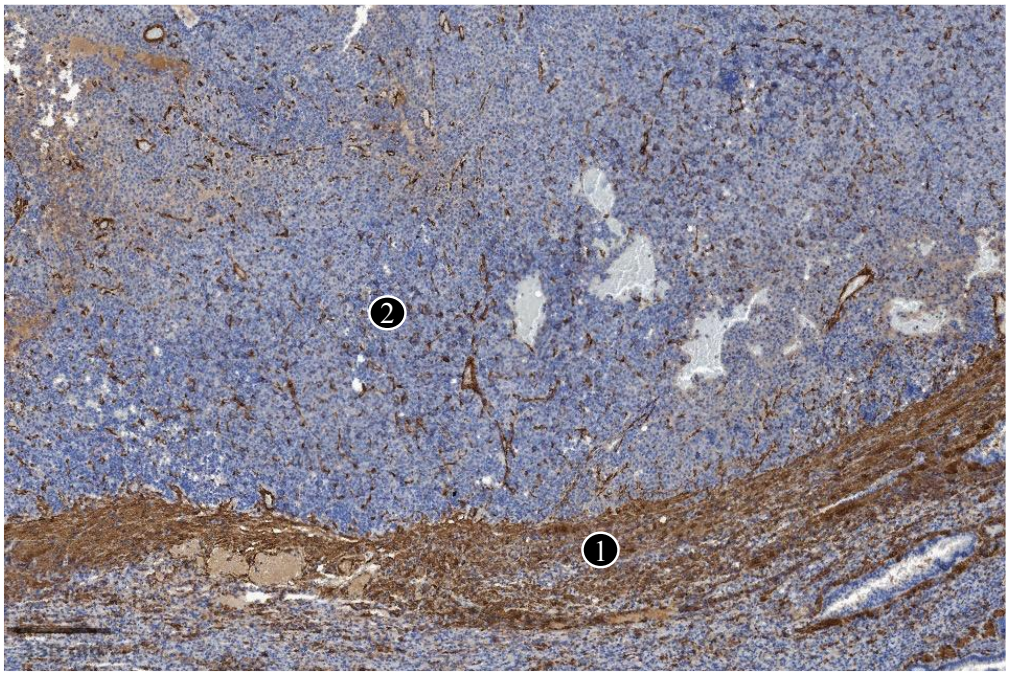

Figure 34: Bile duct mass, α-SMA positive stroma and parenchymal cell clusters (α-SMA, 110x)
1: capsule, 2: mass parenchyma. Note the positive branches in between the cells of the parenchyma.

4.3. Lung masses

4.3.1. Gross appearance

One rounded mass of 4 mm diameter (LM1, Figure 35) was located between the accessory lung lobe and the mediastinum. A second rounded mass of 5-6 mm diameter (LM2, Figure 35) was located between the accessory lung lobe and the right caudal lung lobe. Both masses appeared greyish with brown-red spots, and had soft consistency, with smooth surfaces and fine vasculature. The margins seemed well defined. The surrounding lung tissue was hyperemic and atelectatic.

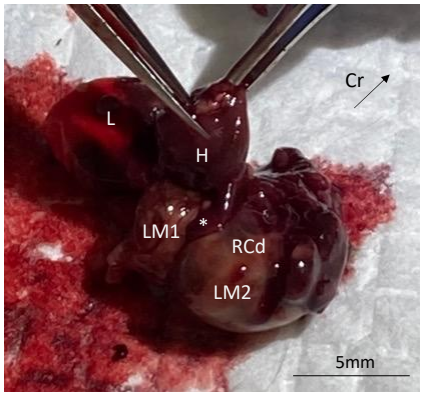

Figure 35: Lung masses gross appearance
Cr: cranial, H: heart, L: left lung lobe, LM1: mass 1, LM2: mass 2, RCd: Right caudal lung lobe, *: accessory lung lobe

4.3.2. Histological features

The two masses showed attachment to the accessory lung lobe. Masses 1 (LM1) and 2 (LM2) were round, 4 mm and 6 mm in diameter respectively, densely cellular and finely capsulated (Figure 36). The masses appeared as structurally arranged clusters of cells without diving septa, and more eosinophilic than the left liver lobe mass. A thin eosinophilic capsule surrounded the two masses. Both masses were very well-vascularised, with numerous large blood vessels, and more numerous smaller blood vessels than the left liver lobe mass. No paler areas suggestive of necrosis were visible (Figure 36).

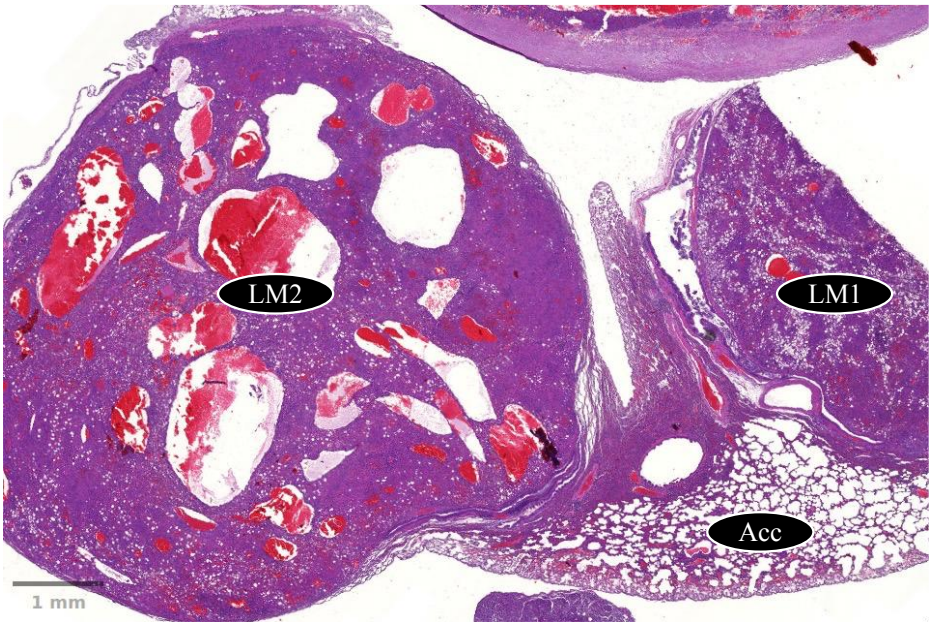

Figure 36: Lung masses, low magnification (H&E, 25x)
LM1: mass 1, LM2: mass 2, Acc: accessory lung lobe

The cells in the masses were more uniform in appearance, with most of them a having polygonal shape. Most cells were relatively large with an extensive eosinophilic cytoplasm. Vacuoles were present in similar manner as in the left liver lobe mass. The cellular margins were clearly defined, unlike the liver mass (Figure 37). The nuclei were round, large and mostly centrally located, containing one or two nucleolus. The chromatin appeared in general granulated. There was marked anisokaryosis, but the anisocytosis was not as common as in the liver mass. Numerous mitotic figures were seen. The normal lung parenchyma in between the masses seemed compressed with loss of alveolar arrangement. The cells in the stroma were spindle-shaped with eosinophilic cytoplasm and elongated basophilic nucleus. Several mitotic figures were found in the capsule but to lesser extent than in the stroma of the liver mass (Figure 37).

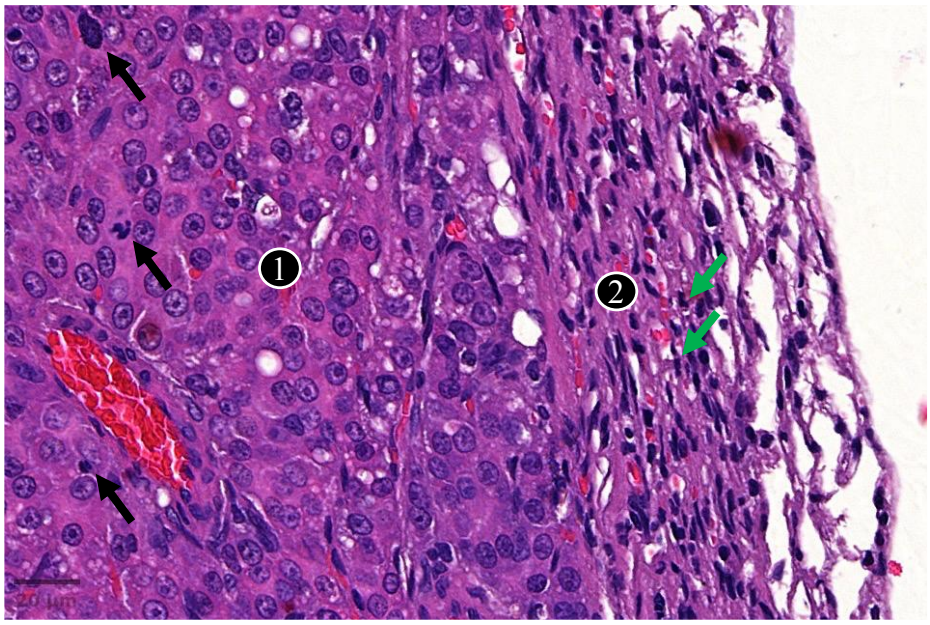

Figure 37: Lung mass 2, cellular morphology and mitotic figures (H&E, 850x)
1: mass parenchyma with tumor hepatic cells, 2: thin capsule of the mass. The black arrows point at mitotic figures in the parenchyma and the green arrows at mitotic figures in the capsule.

Claudin-5 and Factor VII stainings were negative, as in the other masses. Both mass LM1 and LM2 stained positive for HepPar-1, with a more intense and uniform staining in LM1 than in LM2 (Figure 38).

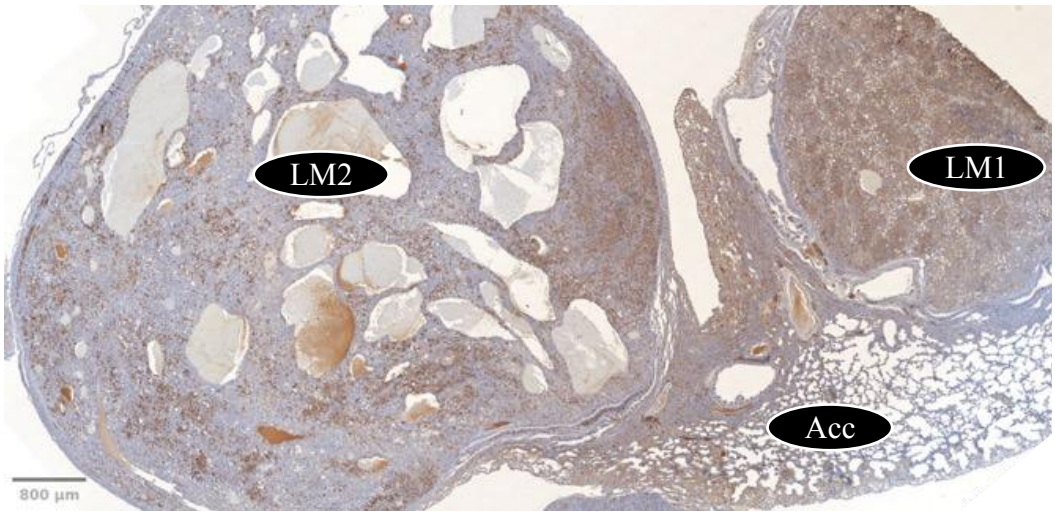

Figure 38: Lung masses, low magnification (HepPar-1, 25x)
LM1: mass 1, LM2: mass 2, Acc: accessory lung lobe. Note how the HepPar-1 staining in mass 1 is more dense and more scattered in mass 2.

The spindle-cells of the capsule stained positive for α-SMA. The staining revealed fine network of positive cells branching inbetween some of the HepPar-1 positive cells, more prominent in LM1 (Figure 39).

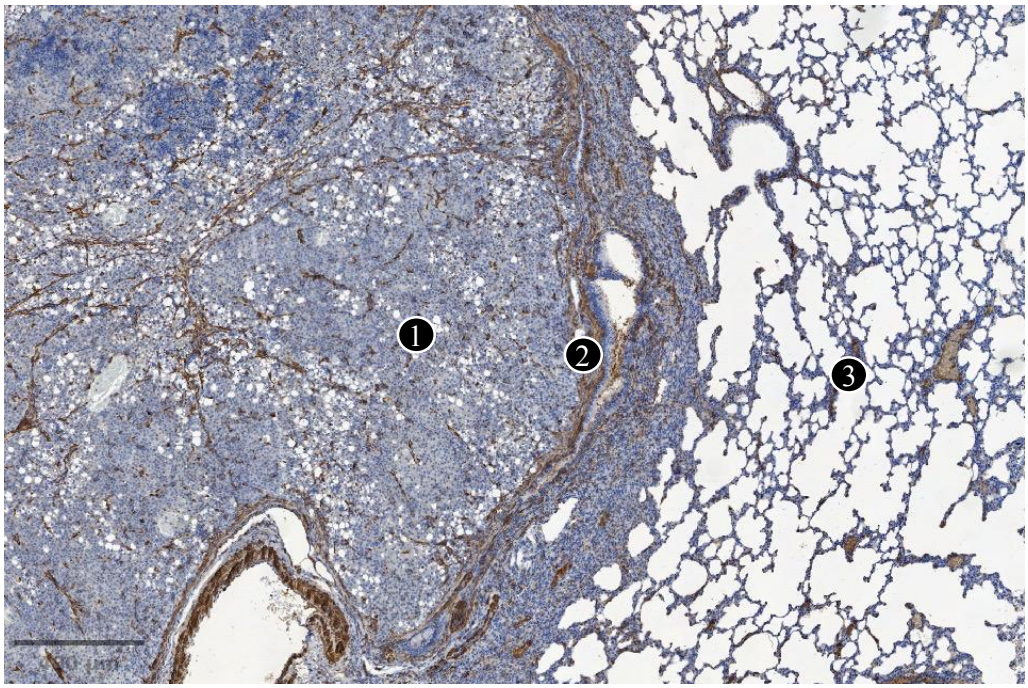

Figure 39: Lung mass 1 (α-SMA, 80x)
1: mass parenchyma, 2: thin capsule, 3: normal lung parenchyma (accessory lobe). Note the fine α-SMA positive network formation in the mass parenchyma.

5. Discussion

In this case study, a dwarf pet rat was presented to a veterinary clinic with respiratory distress. The worsening general condition of the patient led to euthanasia. A necropsy was performed and revealed various masses in the rat's liver, bile duct and lungs.

The nodular masses present in the liver, especially the left liver lobe, macroscopically resembled the description of nodular hepatocellular carcinoma of dogs. Histopathological analysis of the left liver lobe mass revealed HepPar-1 positive pleomorphic cells organized in aggregates without showing specific pattern, and absence of sinusoids. Those cells' microscopical appearance corresponded to hepatocytes with various stages of differentiation, suspicious of tumoral nature of the mass. The large necrotic center of the mass suggested a long going process and was consistent with the relatively large size of the mass. Numerous mitotic figures and poorly to moderately differentiated hepatocytes, including in the blood vessels, suggested malignancy. The negative Claudin-5 and Factor-VIII ruled out hemangiosarcoma. Those macroscopical and histopathological findings were concordant with a nodular hepatocellular carcinoma (HCC) with solid pattern. Even if some cells presented a vacuolized appearance sometimes seen in clear-cell HCC, their amount was not significant enough to conclude this pattern.

The lobulated mass attached to the common bile duct led to a displacement of the duct in the abdomen, making its identification difficult macroscopically. The mass was mostly

composed of HepPar-1 positive cells, with more consistent organization than the liver mass but with still poorly differentiated appearance. This suggested extrahepatic metastasis into the bile duct. The presence of necrotic areas in the mass was consistent with the relatively large size of the tumor.

The gross appearance of the two masses found in the lungs could not at first exclude lesions due to respiratory infection, which are very typical in rats and concordant with the dyspnea of the patient. However, histopathology showed a large amount of HepPar-1 positive cells in both masses, confirming hepatic origin. This suggested that those masses were distant metastases originating from the liver mass. This finding is consistent with the current literature describing the lungs as the most frequent metastatic site of hepatocellular carcinoma in dogs [48, 53].

It is to be noted that other tumorous-looking masses were present in other liver lobes but were not excised during the necropsy. It can be suspected that those masses would be intra-hepatic metastases, but this cannot be confirmed with the collected data.

The presence of several confirmed (bile duct and lungs) and suspected (other liver lobes) metastatic sites showing hepatocyte-like cells corresponds to the highly metastatic potential of solid hepatocellular carcinoma described in dogs [57], and indicates a case of primary liver tumor. As the tumor was invading other organs and had distant metastases, it could be classified as a T3M1 according to the TNM system [58]. The status of the lymph nodes could not be properly assessed in this study. Histologically, the tumor presented marked pleomorphism, prominent nucleoli and solid bizarre pattern, and can hence be categorized as grade IV [58–60]. The rest of the unaffected liver tissue appeared healthy both macroscopically and histologically, which could indicate a spontaneous hepatocellular carcinoma. However, precise etiology could not be established. In the literature, HCC origin in domestic animals is often unknown [49, 53].

The numerous α-SMA positive cells in the stroma and parenchyma of the different masses resembled myofibroblasts. They were however more frequent, more differentiated and more infiltrative in the liver mass, which suggests that they are of hepatic origin. As their cytoplasm presented projections forming a fine network, they are likely to be activated hepatic stellate cells (HSC) [42]. However, desmin staining should be used to confirm this [33]. Their large amount and appearance are consistent with either HSC hyperplasia or tumor. To confirm HSC tumor, antigen Kiel-67 (Ki-67) staining highlighting proliferating cells [72] and calculation of the mitotic index, could be used.

Interestingly, hepatic stellate cells have been described as tumorigenic in the literature [45], and their proliferation could have enhanced the metastatic potential of the hepatocellular carcinoma in this dwarf rat.

The present study describes a grade IV spontaneous primary hepatocellular carcinoma with solid pattern, in a dwarf pet rat. Even though rats are known to be prone to tumors, liver tumors in rats are rarely documented and mostly seen in laboratory rats after artificial induction.

In the current veterinary literature, liver tumors in pet rats are barely mentioned and are considered extremely rare [2]. To the best of the author's knowledge, spontaneous hepatocellular carcinoma in a pet rat has not yet been described. This case study is hoped to enrich the veterinary knowledge about companion rat liver diseases and encourage more detailed clinical investigation, including blood analysis and ultrasound of the dyspneic patient.

6. Summary

Rats, and even more dwarf rats, are still considered unsual pets but their popularity is increasing and understanding them as patients is essential. They are known to be prone to tumors and are used in oncology research for this reason. While mammary gland tumors are common in both laboratory and pet rats, liver tumors are considered very rare and little literature is available. Hence, this study aims to enhance veterinary knowledge about rats liver tumors. It documents the pathological findings in a dwarf pet rat presented for dyspnea and lethargy and euthanised due to poor prognosis. Necropsy revealed several nodular lesions in different liver lobes, lungs and common bile duct. From those, four lesions were analyzed with histopathology: one from the left liver lobe, one from the common bile duct and two from the lungs. All four masses presented numerous HepPar-1 positive cells, with various degree of differentiation. Histological findings of the left liver lobe were consistent with a spontaneous solid hepatocellular carcinoma with vascular invasion. The lungs and common bile duct masses could be determined as metastatic sites of the primary liver tumor. The speading to neighouring organs with distant metastases, presence of marked cellular pleomorphism and solid pattern allowed to categorize a grade IV hepatocellular carcinoma. The use of α-SMA staining showed an associated myofibroblast-like cells proliferation which could be consistent with either hepatic stellate cell hyperplasia or tumor, but could not confirmed. This case study provides histopathological documentation of a rare liver tumor in a dwarf pet rat, which, to the best of the author's knowledge, had not yet been described. It is hoped to enrich veterinary literature and encourage deeper investigation of the dyspneic pet rat.

7. References

1. Frohlich J (2020) Diseases of rats. In: Ferrets, Rabbits, and Rodents Clinical Medicine and Surgery, 4th Edition. Elsevier Inc., Missouri, pp 361–365

2. Turner PV, Brash ML, Smith DA (2017) Rats. In: Pathology of Small Mammal Pets. John Wiley & Sons, Inc., Hoboken, pp 225–276

3. Vergneau-Grosset C, Keel MK, Goldsmith D, Kass PH, Paul-Murphy J, Hawkins MG (2016) Description of the prevalence, histologic characteristics, concomitant abnormalities, and outcomes of mammary gland tumors in companion rats (Rattus norvegicus): 100 cases (1990–2015). Journal of the American Veterinary Medical Association 249:1170–1179. https://doi.org/10.2460/javma.249.10.1170

4. Planas-Silva MD, Rutherford TM, Stone MC (2008) Prevention of age-related spontaneous mammary tumors in outbred rats by late ovariectomy. Cancer Detection and Prevention 32:65–71. https://doi.org/10.1016/j.cdp.2008.01.004

5. Thordarson G, Semaan S, Low C, Ochoa D, Leong H, Rajkumar L, Guzman RC, Nandi S, Talamantes F (2004) Mammary tumorigenesis in growth hormone deficient spontaneous dwarf rats; effects of hormonal treatments. Breast Cancer Res Treat 87:277–290. https://doi.org/10.1007/s10549-004-9504-2

6. Swanson SM, Unterman TG (2002) The growth hormone-deficient Spontaneous Dwarf rat is resistant to chemically induced mammary carcinogenesis. Carcinogenesis 23:977–982. https://doi.org/10.1093/carcin/23.6.977

7. Sasaki T, Tahara S, Shinkai T, Kuramoto K, Matsumoto S, Yanabe M, Takagi S, Kondo H, Kaneko T (2013) Lifespan extension in the spontaneous dwarf rat and enhanced resistance to hyperoxia-induced mortality. Experimental Gerontology 48:457–463. https://doi.org/10.1016/j.exger.2013.02.015

8. Sharp P, Villano JS (2012) The Laboratory Rat, 2nd Edition. CRC Press, Boca Raton

9. Takeuchi T, Suzuki H, Sakurai S, Nogami H, Okuma S, Ishikawa H (1990) Molecular Mechanism of Growth Hormone (GH) Deficiency in the Spontaneous Dwarf Rat: Detection of Abnormal Splicing of GH Messenger Ribonucleic Acid by the Polymerase Chain Reaction*. Endocrinology 126:31–38. https://doi.org/10.1210/endo-126-1-31

10. Okuma S (1984) Study of Growth Hormone in Spontaneous Dwarf Rat. Folia Endocrinol 60:1005–1014. https://doi.org/10.1507/endocrine1927.60.8_1005

11. Kuramoto K, Tahara S, Sasaki T, Matsumoto S, Kaneko T, Kondo H, Yanabe M, Takagi S, Shinkai T (2010) Spontaneous dwarf rat: A novel model for aging research. Geriatrics & Gerontology International 10:94–101. https://doi.org/10.1111/j.1447-0594.2009.00559.x

12. AFRMA - Colors & Coats - Dwarf Rat Info; Blue Genes Influence Size?; Small Rats. https://www.afrma.org/c-c_dwarfsmallrat.htm. Accessed 11 Sep 2023

13. National Fancy Rat Society - NFRS. https://www.nfrs.org/breeding_varieties.html. Accessed 18 Dec 2021

14. Andersen ML, Lee KS, Guindalini C, Leite WA, Bignotto M (2009) Altered Sleep Patterns and Physiologic Characteristics in Spontaneous Dwarf Rats. Comparative Medicine 59:

15. Yamaza H, Komatsu T, Chiba T, Toyama H, To K, Higami Y, Shimokawa I (2004) A transgenic dwarf rat model as a tool for the study of calorie restriction and aging. Experimental Gerontology 39:269–272. https://doi.org/10.1016/j.exger.2003.11.001

16. Shen Q, Lantvit DD, Lin Q, Li Y, Christov K, Wang Z, Unterman TG, Mehta RG, Swanson SM (2007) Advanced Rat Mammary Cancers Are Growth Hormone Dependent. Endocrinology 148:4536–4544. https://doi.org/10.1210/en.2007-0513

17. Hocker SE, Eshar D, Wouda RM (2017) Rodent Oncology. Veterinary Clinics of North America: Exotic Animal Practice 20:111–134. https://doi.org/10.1016/j.cvex.2016.07.006

18. Cohen LA, Chan PC, Wynder EL (1981) The role of a high-fat diet in enhancing the development of mammary tumors in ovariectomized rats. Cancer 47:66–71. https://doi.org/10.1002/1097-0142(19810101)47:1<66::AID-CNCR2820470113>3.0.CO;2-M

19. Park S, Sohn S, Kineman R (2004) Fasting-induced changes in the hypothalamic-pituitary-GH axis in the absence of GH expression: lessons from the spontaneous dwarf rat. Journal of Endocrinology 180:369–378. https://doi.org/10.1677/joe.0.1800369

20. Davies JS, Gevers EF, Stevenson AE, Coschigano KT, El-Kasti MM, Bull MJ, Elford C, Evans BAJ, Kopchick JJ, Wells T (2007) Adiposity profile in the dwarf rat: an unusually lean model of profound growth hormone deficiency. American Journal of Physiology-Endocrinology and Metabolism 292:E1483–E1494. https://doi.org/10.1152/ajpendo.00417.2006

21. AFRMA - The History of Fancy Rats. https://www.afrma.org/historyrat.htm. Accessed 11 Apr 2022

22. Taylor J (2007) “Ratatouille” inspires a run on rats at British pet shops. The Independent

23. Chantry C (2007) C’est la ruée sur les rats. Le Parisien

24. Treuting PM, Dintzis SM, Montine KS (2018) Comparative anatomy and histology: a mouse, rat, and human atlas, Second edition. Academic Press, London San Diego Cambridge, MA Kidlington

25. Stan FG (2018) Comparative Study of the Liver Anatomy in the Rat, Rabbit, Guinea Pig and Chinchilla. BUASVMCN-VM 75:33. https://doi.org/10.15835/buasvmcn-vm:002717

26. Maynard RL, Downes N (2019) Anatomy and Histology of the Laboratory Rat in Toxicology and Biomedical Research. Elsevier, Academic Press, London

27. Eurell JA, Frappier BL (2013) Dellmann’s Textbook of Veterinary Histology, 6th ed. Wiley, Philadelphia

28. Zachary JF (2017) Pathologic basis of veterinary disease, Sixth edition. Elsevier, St. Louis, Missouri

29. (2020) Normal Liver Histology 101 | AASLD. https://www.aasld.org/liver-fellow-network/core-series/pathology-pearls/normal-liver-histology-101. Accessed 15 Oct 2023

30. Panwar A, Das P, Tan LP (2021) 3D Hepatic Organoid-Based Advancements in LIVER Tissue Engineering. Bioengineering 8:185. https://doi.org/10.3390/bioengineering8110185

31. Chen F, Schönberger K, Tchorz JS (2023) Distinct hepatocyte identities in liver homeostasis and regeneration. JHEP Reports 5:100779. https://doi.org/10.1016/j.jhepr.2023.100779

32. IJzer J, Roskams T, Molenbeek RF, Ultee T, Penning LC, Rothuizen J, Van Den Ingh TS (2006) Morphological characterisation of portal myofibroblasts and hepatic stellate cells in the normal dog liver. Comp Hepatol 5:7. https://doi.org/10.1186/1476-5926-5-7

33. Maher JJ (1989) Fat-storing cells and myofibroblasts: One cell or two? Hepatology 9:903–904. https://doi.org/10.1002/hep.1840090621

34. Senoo H (2004) Structure and function of hepatic stellate cells. Medical Electron Microscopy 37:3–15. https://doi.org/10.1007/s00795-003-0230-3

35. Balabaud C (2004) The role of hepatic stellate cells in liver regeneration. Journal of Hepatology 40:1023–1026. https://doi.org/10.1016/j.jhep.2004.04.003

36. Friedman SL (2008) Hepatic Stellate Cells: Protean, Multifunctional, and Enigmatic Cells of the Liver. Physiological Reviews 88:125–172. https://doi.org/10.1152/physrev.00013.2007

37. Gulubova MV Ito cell morphology, α-smooth muscle actin and collagen type IV expression in the liver of patients with gastric and colorectal tumors

38. Knittel T, Kobold D, Piscaglia F, Saile B, Neubauer K, Mehde M, Timpl R, Ramadori G (1999) Localization of liver myofibroblasts and hepatic stellate cells in normal and diseased rat livers: distinct roles of (myo-)fibroblast subpopulations in hepatic tissue repair. Histochemistry and Cell Biology 112:387–401. https://doi.org/10.1007/s004180050421

39. Mann DA, Marra F (2010) Fibrogenic signalling in hepatic stellate cells. Journal of Hepatology 52:949–950. https://doi.org/10.1016/j.jhep.2010.02.005

40. Yin C, Evason KJ, Asahina K, Stainier DYR (2013) Hepatic stellate cells in liver development, regeneration, and cancer. J Clin Invest 123:1902–1910. https://doi.org/10.1172/JCI66369

41. Mabuchi A (2004) Role of hepatic stellate cell/hepatocyte interaction and activation of hepatic stellate cells in the early phase of liver regeneration in the rat. Journal of Hepatology 40:910–916. https://doi.org/10.1016/j.jhep.2004.02.005

42. Andez AM, Amenta PS (1995) The extracellular matrix in hepatic regeneration. FASEB j 9:1401–1410. https://doi.org/10.1096/fasebj.9.14.7589981

43. Krizhanovsky V, Yon M, Dickins RA, Hearn S, Simon J, Miething C, Yee H, Zender L, Lowe SW (2008) Senescence of Activated Stellate Cells Limits Liver Fibrosis. Cell 134:657–667. https://doi.org/10.1016/j.cell.2008.06.049

44. Fasbender F, Widera A, Hengstler JG, Watzl C (2016) Natural Killer Cells and Liver Fibrosis. Front Immunol 7:. https://doi.org/10.3389/fimmu.2016.00019

45. Barry AE, Baldeosingh R, Lamm R, Patel K, Zhang K, Dominguez DA, Kirton KJ, Shah AP, Dang H (2020) Hepatic Stellate Cells and Hepatocarcinogenesis. Front Cell Dev Biol 8:709. https://doi.org/10.3389/fcell.2020.00709

46. Debing Y, Mishra N, Verbeken E, Ramaekers K, Dallmeier K, Neyts J (2016) A rat model for hepatitis E virus. Disease Models & Mechanisms dmm.024406. https://doi.org/10.1242/dmm.024406

47. Maneerat Y, Clayson ET, Myint KSA, Young GD, Innis BL (1996) Experimental infection of the laboratory rat with the hepatitis E virus. J Med Virol 48:121–128. https://doi.org/10.1002/(SICI)1096-9071(199602)48:2<121::AID-JMV1>3.0.CO;2-B

48. Maxie MG (2016) Jubb, Kennedy, and Palmer's pathology of domestic animals, Sixth edition. Elsevier, St. Louis, Missouri

49. Meuten DJ (2002) Tumors in domestic animals, 4th ed. Iowa State Press, Ames

50. Bruix J, Boix L, Sala M, Llovet JM (2004) Focus on hepatocellular carcinoma. Cancer Cell 5:215–219. https://doi.org/10.1016/S1535-6108(04)00058-3

51. Balogh J, Victor D, Asham EH, Burroughs SG, Boktour M, Saharia A, Li X, Ghobrial M, Monsour H (2016) Hepatocellular carcinoma: a review. JHC Volume 3:41–53. https://doi.org/10.2147/JHC.S61146

52. Kurma K, Manches O, Chuffart F, Sturm N, Gharzeddine K, Zhang J, Mercey-Ressejac M, Rousseaux S, Millet A, Lerat H, Marche PN, Macek Jilkova Z, Decaens T (2021) DEN-Induced Rat Model Reproduces Key Features of Human Hepatocellular Carcinoma. Cancers 13:4981. https://doi.org/10.3390/cancers13194981

53. Withrow SJ, Vail DM, Page RL (2013) Withrow & MacEwen's small animal clinical oncology, 5th edition. Elsevier, St. Louis, Missouri

54. Suttie AW (2015) Boorman's Pathology of the Rat (2nd Ed.). Reference and Atlas., 2nd Edition. Elsevier, Academic Press, London

55. Barthold SW, Percy DH, Griffey SM (2016) Pathology of laboratory rodents and rabbits, Fourth edition. John Wiley & Sons, Inc, Ames, Iowa

56. Webpathology.com: A Collection of Surgical Pathology Images. https://www.webpathology.com/image.asp?n=43&Case=238. Accessed 15 Oct 2023

57. Gisder DM, Tannapfel A, Tischoff I (2022) Histopathology of hepatocellular carcinoma - when and what. HR. https://doi.org/10.20517/2394-5079.2021.106

58. Marconato L, Sabattini S, Marisi G, Rossi F, Leone VF, Casadei-Gardini A (2020) Sorafenib for the Treatment of Unresectable Hepatocellular Carcinoma: Preliminary Toxicity and Activity Data in Dogs. Cancers 12:1272. https://doi.org/10.3390/cancers12051272

59. Maniscalco L, Varello K, Morello E, Montemurro V, Olimpo M, Giacobino D, Abbamonte G, Gola C, Iussich S, Bozzetta E (2022) Investigating a Prognostic Factor for Canine Hepatocellular Carcinoma: Analysis of Different Histological Grading Systems and the Role of PIVKA-II. Veterinary Sciences 9:689. https://doi.org/10.3390/vetsci9120689

60. Martins-Filho SN, Paiva C, Azevedo RS, Alves VAF (2017) Histological Grading of Hepatocellular Carcinoma—A Systematic Review of Literature. Front Med 4:193. https://doi.org/10.3389/fmed.2017.00193

61. Siddiqui MT, Hossein Saboorian M, Tunc Gokaslan S, Ashfaq R (2002) Diagnostic utility of the HepPar1 antibody to differentiate hepatocellular carcinoma from metastatic carcinoma in fine-needle aspiration samples. Cancer 96:49–52. https://doi.org/10.1002/cncr.10311

62. Fan Z, Van De Rijn M, Montgomery K, Rouse RV (2003) Hep Par 1 Antibody Stain for the Differential Diagnosis of Hepatocellular Carcinoma: 676 Tumors Tested Using Tissue Microarrays and Conventional Tissue Sections. Modern Pathology 16:137–144. https://doi.org/10.1097/01.MP.0000052103.13730.20

63. Shiran MS, Isa MR, Sherina MS, Rampal L, Hairuszah I, Sabariah AR (2006) The utility of Hepatocyte Paraffin 1 antibody in the immunohistological distinction of hepatocellular carcinoma from cholangiocarcinoma and metastatic carcinoma

64. Conference 20 - 2018 Case: 4 20180404. https://www.askjpc.org/wsco/wsc_showcase2.php?id=RXRFRC9mNVZNUWRyZ092MDdtWDM0QT09. Accessed 1 Nov 2023

65. Pathology Outlines - HepPar1. https://www.pathologyoutlines.com/topic/stainsheppar1.html. Accessed 30 Oct 2023

66. Pathology Outlines - Actin, alpha smooth muscle type. https://www.pathologyoutlines.com/topic/stainsalphasmoothmuscleactin.html. Accessed 30 Oct 2023

67. Nakatani T, Honda E, Hayakawa S, Sato M, Satoh K, Kudo M, Munakata H (2008) Effects of decorin on the expression of α-smooth muscle actin in a human myofibroblast cell line. Mol Cell Biochem 308:201–207. https://doi.org/10.1007/s11010-007-9629-9

68. Miettinen M, Sarlomo-Rikala M, Wang Z-F (2011) Claudin-5 as an Immunohistochemical Marker for Angiosarcoma and Hemangioendotheliomas. American Journal of Surgical Pathology 35:1848–1856. https://doi.org/10.1097/PAS.0b013e318229a401

69. Pathology Outlines - Claudins. https://www.pathologyoutlines.com/topic/stainsclaudins.html. Accessed 30 Oct 2023

70. Comper F, Antonello D, Beghelli S, Gobbo S, Montagna L, Pederzoli P, Chilosi M, Scarpa A (2009) Expression Pattern of Claudins 5 and 7 Distinguishes Solid-pseudopapillary From Pancreatoblastoma, Acinar Cell and Endocrine Tumors of the Pancreas. American Journal of Surgical Pathology 33:768–774. https://doi.org/10.1097/PAS.0b013e3181957bc4

71. Factor VIII related antigen. https://www.pathologyoutlines.com/topic/stainsfactorviii.html. Accessed 30 Oct 2023

72. Sun X, Kaufman PD (2018) Ki-67: more than a proliferation marker. Chromosoma 127:175–186. https://doi.org/10.1007/s00412-018-0659-8

Acknowledgments

Firstly, I would like to acknowledge and thank my thesis supervisor, Pr. Mándoki, professor and head of the Department of Pathology of the UVMB, for her guidance and for giving me a chance to write this thesis.

Secondly I would like to thank both Dr. Szilasi, assistant professor at Department of Pathology of the UVMB, for her help and insight regarding the histopathology results, and Dr. Balka, associate professor at the Department of Pathology of the UVMB, for his work on the samples provided.

Lastly I would like to thank Elsa, my future colleague, for all the patience and help she provided me. Without her I wouldn't be where I am today.

Thesis progress report for veterinary students

Name of student: **Sigurðarson Björn Benedikt**
Neptun code of the student: **JWHXXB**
Name and title of the supervisor: **Pr. Míra Mándoki, Professor and head of department**
Department: **Department of Pathology**
Thesis title: **Hepatocellular carcinoma in a dwarf pet rat: A case study**

Consultation – 1st semester

	Timing			Topic / Remarks of the supervisor	Signature of the supervisor
	year	month	day		
1.	2023	07	14	Thesis topic discussion	
2.	2023	07	20	Thesis writing plan	
3.	2023	07	23	Review of introduction	
4.	2023	07	26	Review of material and method	
5.	2023	07	30	Literature review plan	

Grade achieved at the end of the first semester: .....excellent (5).....

Consultation – 2nd semester

	Timing			Topic / Remarks of the supervisor	Signature of the supervisor
	year	month	day		
1.	2023	09	30	Correction of literature review	
2.	2023	10	15	Discussion of histopathology results Further correction of literature review	
3.	2023	10	26	Review of main study results	
4.	2023	11	2	Preparation for the plagarism check	
5.	2023	11	14	Finalization of thesis paper	

Grade achieved at the end of the second semester: ..... excellent (5).....

The thesis meets the requirements of the Study and Examination Rules of the University and the Guide to Thesis Writing.
I accept the thesis and find suitable to defence,

.....
signature of the supervisor

Signature of the student: .....
Signature of the secretary of the department: .....
Date of handing the thesis in: 2023/11/16

Supervisor's consent form

I hereby confirm that I am familiar with the content of the thesis entitled „**Hepatic cellular carcinoma in a dwarf pet rat: a case study**" written by Björn Benedikt Sigurðarson, which I deem suitable for submission and defence.

Date: 14th of November 2023

.....

Dr. Mándoki, Míra

Pathology Department